SUPPORTING INFORMATION for

Boronate Esters for the Binding and Detection of Low Molecular Weight Volatile Amines

Xiaoning Li, James Boyt, Min Cai, Steven Sloope, Luke T. Lackovic, Mark D. Smith and John J. Lavigne*

Department of Chemistry & Biochemistry, 631 Sumter Street, University of South Carolina, Columbia, SC 29208

Fax: +1-803-777-9521; Tel: +1-803-777-2295; E-mail: lavigne@sc.edu

Contents

Instrumentation	S2
Binding Constants	S2
Cooperativity Interaction Parameters	S3
X-Ray Structure Determination	S4
Solution Preparation	S6
Reversibility Studies	S7
Synthesis and Characterization	S11
NMR and HRMS for Compounds **1**-**4**	S13
Absorption Titration Spectra and Data Fitting	S26
Mole Ratio Stoichiometry Plot	S39
References	S40

Instrumentation

Solution phase ^{1}H NMR and ^{13}C NMR, and ^{11}B NMR spectra were collected on a Bruker Avance III-HD (300 MHz for ^{1}H and 100 MHz for ^{13}C, and 400 mHz for ^{11}B). UV-vis absorbance studies were performed using a Beckman Coulter 640 DU Spectrophotometer and quartz cuvettes from Starna. Fluorescence emission studies were performed using a Cary Eclipse Fluorescence Spectrophotometer. X-ray diffraction data was collected at Bruker SMART APEX diffractometer Mo Kα radiation.

Binding Constants

Table S1: Binding constants K_{a1}.

		$logK_{a1}$				**Standard Deviation of $logK_{a1}$**		
Analyte	**pK_b**	**1**	**2**	**3**	4	**1**	**2**	**3**
***n*BuNH$_2$**	3.41	5.10	5.19	5.39	3.95	*0.12*	*0.02*	*0.06*
***i*PrNH$_2$**	3.37	4.27	4.82	4.58	3.32	*0.09*	*0.06*	*0.04*
***i*Pr$_2$NH**	2.95	4.74	5.28	5.15	3.29	*0.01*	*0.07*	*0.12*
***i*Pr$_2$EtN**	2.60	5.71	6.19	5.99	3.63	*0.04*	*0.18*	*0.01*

Table S2: Binding constants K_{a2}

	$logK_{a2}$				**Standard Deviation of $logK_{a2}$**		
Analyte	**1**	**2**	**3**	**4**	**1**	**2**	**3**
***n*BuNH$_2$**	3.28	3.31	3.39	2.98	0.16	0.02	0.01
***i*PrNH$_2$**	3.10	3.49	3.30	2.92	0.05	0.03	0.02
***i*Pr$_2$NH**	3.72	3.49	3.77	3.00	0.17	0.17	0.23
***i*Pr$_2$EtN**	3.92	4.04	3.51	2.84	0.17	0.17	0.03

Table S3: Interaction Parameter, α

	α			
Analyte	**1**	**2**	**3**	**4**
***n*BuNH$_2$**	0.060	0.053	0.039	0.43
***i*PrNH$_2$**	0.27	0.19	0.21	1.59
***i*Pr$_2$NH**	0.38	0.065	0.17	2.07
***i*Pr$_2$EtN**	0.065	0.028	0.013	0.65

X-Ray Structure Determination, $C_{16}H_{10}B_2O_4S$ (Compound 1)

X-ray intensity data from a colorless needle crystal were measured at 100(2) K using a Bruker SMART APEX diffractometer (Mo Kα radiation, λ = 0.71073 Å).[1] The raw area detector data frames were reduced and corrected for absorption effects with the SAINT+ and SADABS programs.[1] Final unit cell parameters were determined by least-squares refinement of 5343 reflections from the data set. Direct methods structure solution, difference Fourier calculations and full-matrix least-squares refinement against F^2 were performed with SHELXTL.[2]

The compound crystallizes in the space group C2/c. The asymmetric unit consists of one molecule. Non-hydrogen atoms were refined with anisotropic displacement parameters. Hydrogen atoms were placed in geometrically idealized positions and included as riding atoms.

X-Ray Structure Determination, $[N((CH_2)_3CH_3)_4]_2(C_{16}H_{10}B_2F_2O_4S)\cdot CDCl_3$ (Compound 1-$2F^-$)

X-ray intensity data from a colorless, square blocklike crystal were measured at 100(2) K using a Bruker SMART APEX diffractometer (Mo Kα radiation, λ = 0.71073 Å).[1] Raw area detector data frame processing was performed with the SAINT+ program.[1] Final unit cell parameters were determined by least-squares refinement of 7683 reflections from the data set. Direct methods structure solution, difference Fourier calculations and full-matrix least-squares refinement against F^2 were performed with SHELXTL.[2]

The compound crystallizes in the space group $P2_1/c$ as determined by the pattern of systematic absences in the intensity data. The asymmetric unit consists of two independent $[N((CH_2)_3CH_3)_4]^+$ cations, one $C_{16}H_{10}B_2F_2O_4S^-$ anion and one $CDCl_3$ molecule of crystallization. All species are located on positions of general crystallographic symmetry. Non-hydrogen atoms were refined with anisotropic displacement parameters. Hydrogen atoms were placed in geometrically idealized positions and included as riding atoms.

Table S4: Crystallographic data for compounds **1** and **1**-2F

	1	**1**-2F
Empirical formula	$C_{16}H_{10}B_2O_4S$	$C_{49}H_{82}B_2Cl_3DF_2N_2O_4S$
Formula weight	319.92	963.21
Temperature	100(2) K	100(2) K
Wavelength	0.71073 Å	0.71073 Å
Crystal system	Monoclinic	Monoclinic
Space group	C 2/c	P 21/c
Unit cell dimensions	a = 22.971(2) Å b = 4.8498(4) Å c = 26.049(2) Å α = 90° β = 92.150(2)° γ = 90°	a = 22.0779(12) Å b = 14.3138(7) Å c = 17.3460(9) Å a= 90° b= 104.5180(10)° γ = 90°
Volume	2899.9(4) $Å^3$	5306.6(5) $Å^3$
Z	8	4
Density (calculated)	1.466 Mg/m^3	1.206 Mg/m^3
Absorption coefficient	0.239 mm^{-1}	0.261 mm^{-1}
F(000)	1312	2072
Crystal size	0.48×0.16×0.10mm^3	0.46×0.40×0.22mm^3
Theta range for data collection	1.56 to 26.40°	1.71 to 26.41°
Index ranges	-28<=h<=28, -6<=k<=6, -32<=l<=32	-27<=h<=27, -17<=k<=17, -21<=l<=21
Reflections collected	26053	66206
Independent reflections	2962 [R(int) = 0.0403]	10874 [R(int) = 0.0588]
Completeness to theta = 26.4°	99.9 %	99.9 %
Absorption correction	Semi-empirical from equivalents	None
Max. and min. transmission	1.0000 and 0.9120	
Refinement method	Full-matrix least-squares on F^2	Full-matrix least-squares on F^2
Data/restraints/ parameters	2962/0/208	10874/0/576
Goodness-of-fit on F^2	1.063	1.010
Final R indices [I>2sigma(I)]	R1 = 0.0374, wR2 = 0.0932	R1 = 0.0471, wR2 = 0.1197
R indices (all data)	R1 = 0.0411, wR2 = 0.0960	R1 = 0.0664, wR2 = 0.1292
Largest diff. peak and hole	0.400 and -0.276 $e.Å^{-3}$	0.569 and -0.469 $e.Å^{-3}$

Solution Preparation

Compound **1** was dissolved in dry dichloromethane to prepare 4 mM stock solutions. The stock solution was diluted to 0.035 mM working solution by dichloromethane for titration studies with nBuNH$_2$, iPrNH$_2$ and iPr$_2$NH. The sensor working solution for iPr$_2$EtN was prepared as 0.02 mM by the same stock solution. Stock solutions (100 mM) for each amine analyte were made in dichloromethane, and diluted to 10 mM for nBuNH$_2$, iPrNH$_2$ and iPr$_2$NH, to 5 mM for iPr$_2$EtN for the working solution. Solutions for compound **2-4** were prepared by similar procedures for the absorbance titration studies.

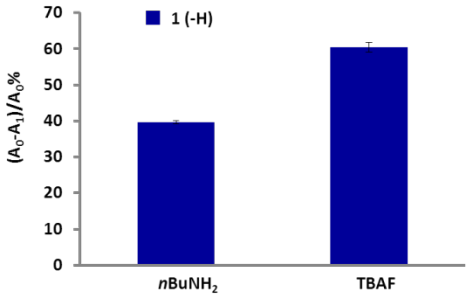

Fig. S1. Normalized absorbance response of **1** at 292 nm with an addition of 2 equivalents of nBuNH$_2$ and TBAF.

Reversibility Studies

To demonstrate the reversibility of bis(dioxaborole)s binding fluoride, excess trimethylsilyl chloride (TMSCl) was added to the fluoride complexes to scavenge fluoride. Meanwhile, bis(dioxaborole)s and chloride were released (Fig. 2a). Upon the addition of TMSCl to fluoride complexes, the absorption maxima of **1** and **3** redshifts back and absorbance restores (Fig. 2). These results indicate the reversible interaction between borole moieties on bis(dioxaborole)s and fluoride and demonstrate the borole stability.

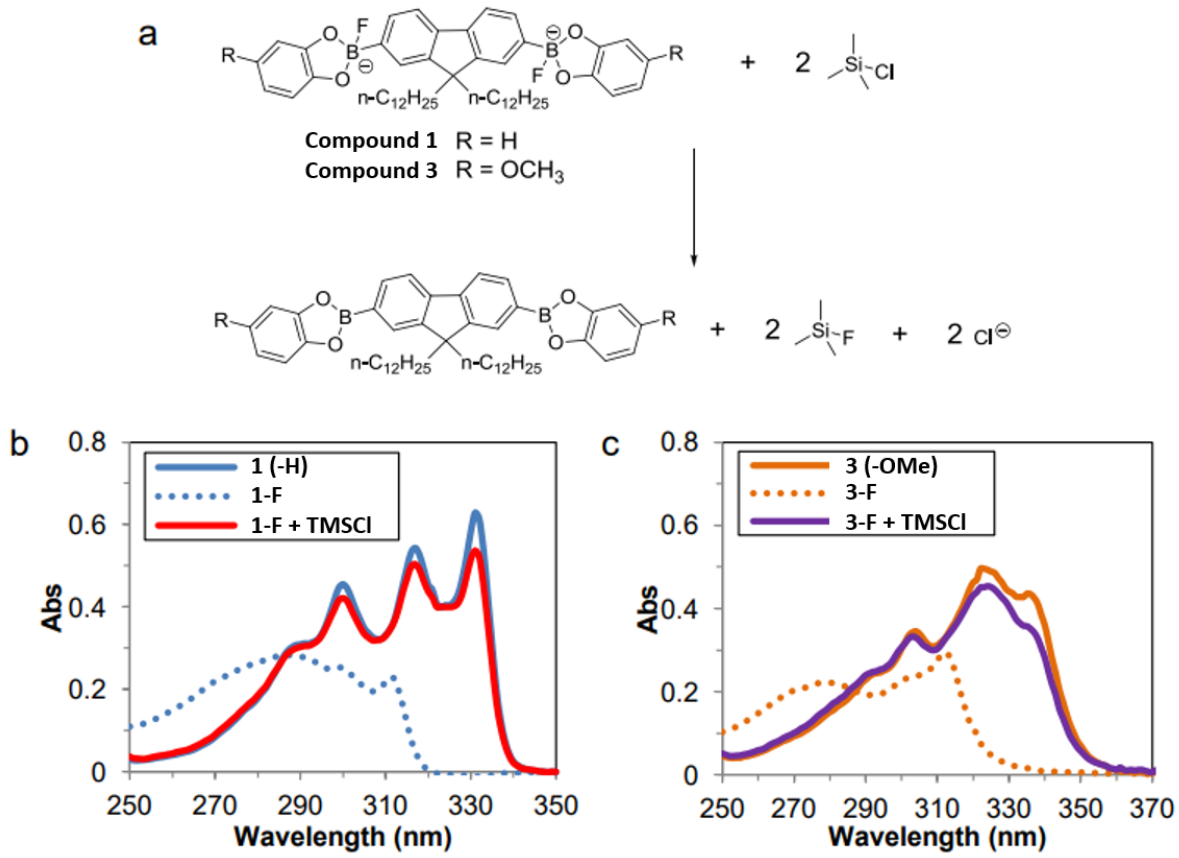

Fig. S2. (a) Representation of fluoride-bis(dioxaborole) complexes reacting with TMSCl. Absorption spectra of 1×10^{-5} M bis(dioxaborole)s (b) **1**(-H), and (c) **3**(-OCH_3) in the presence of 2×10-5 M TBAF upon the addition of excess TMSCl in CH_2Cl_2.

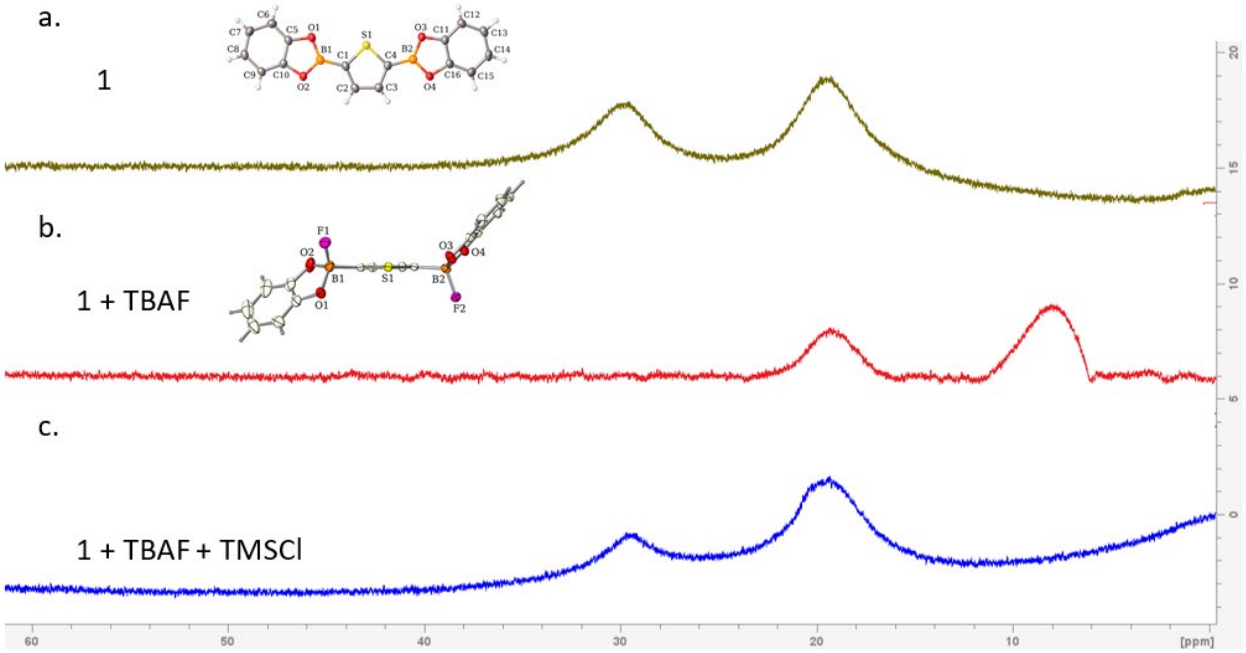

Fig. S3. ^{11}B NMR spectra of **1** using an isolated internal reference standard of boric acid (19.3 ppm). (a) Free **1** in $CDCl_3$ (29.6 ppm). (b) **1** with two equivalents of TBAF (1:1 mole equivalents B:F) in $CDCl_3$. This interaction shifts the ^{11}B resonance to 8.0 ppm. (c) **1** with two equivalents of TBAF (1:1 mole equivalents B:F) and excess of TMSCl in $CDCl_3$, the TMSCl competes for the F^- ion, regenerating free **1** (29.6 ppm).

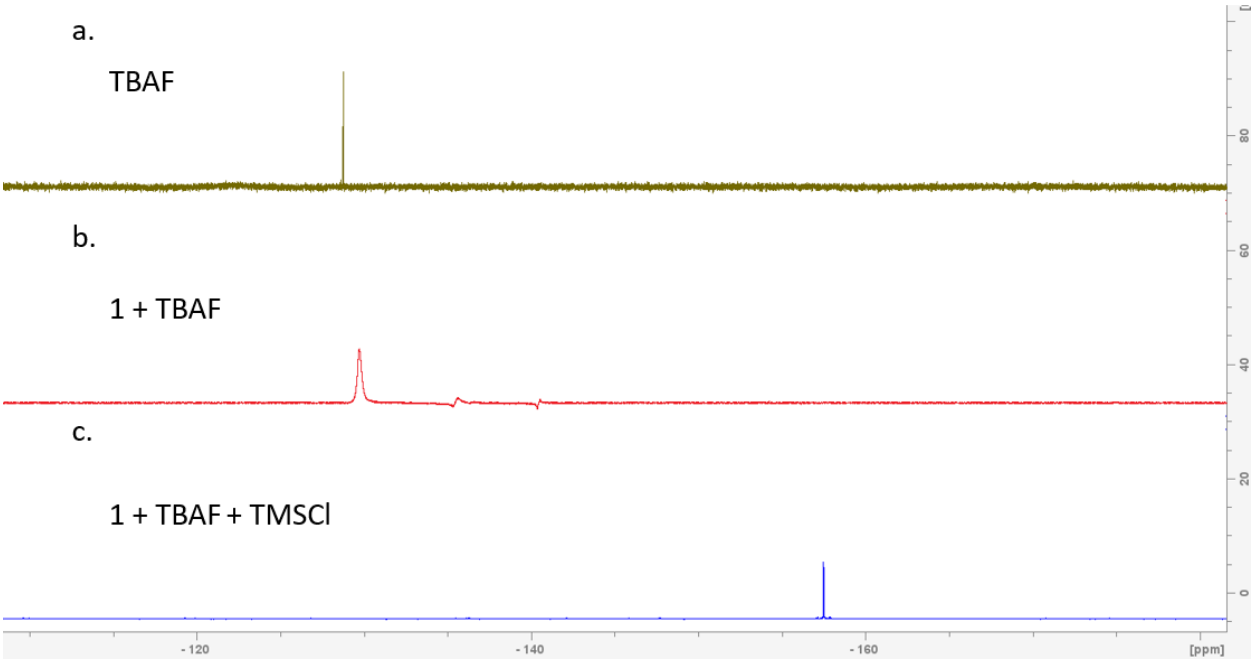

Fig. S4. ^{19}F NMR spectra of TBAF (free F^-) in $CDCl_3$ displays a narrow peak at -128.75 ppm. (b) **1** with two equivalents of TBAF (1:1 mole equivalents B:F) in $CDCl_3$. This interaction shifts the ^{19}F resonance to -129.70 ppm and significantly broadens it (1.1 ppm baseline width vs 0.02 ppm baseline width of free F^- resonance). The expected quadruplet of the B-F ^{19}F signal is not resolved, one broad singlet is observed instead. (c) **1** with two equivalents of TBAF (1:1 mole equivalents B:F) and excess of TMSCl in $CDCl_3$, the TMSCl scavenges the F^- ion, shifting the ^{19}F resonance to -157.47 ppm (peak baseline width = 0.05 ppm).

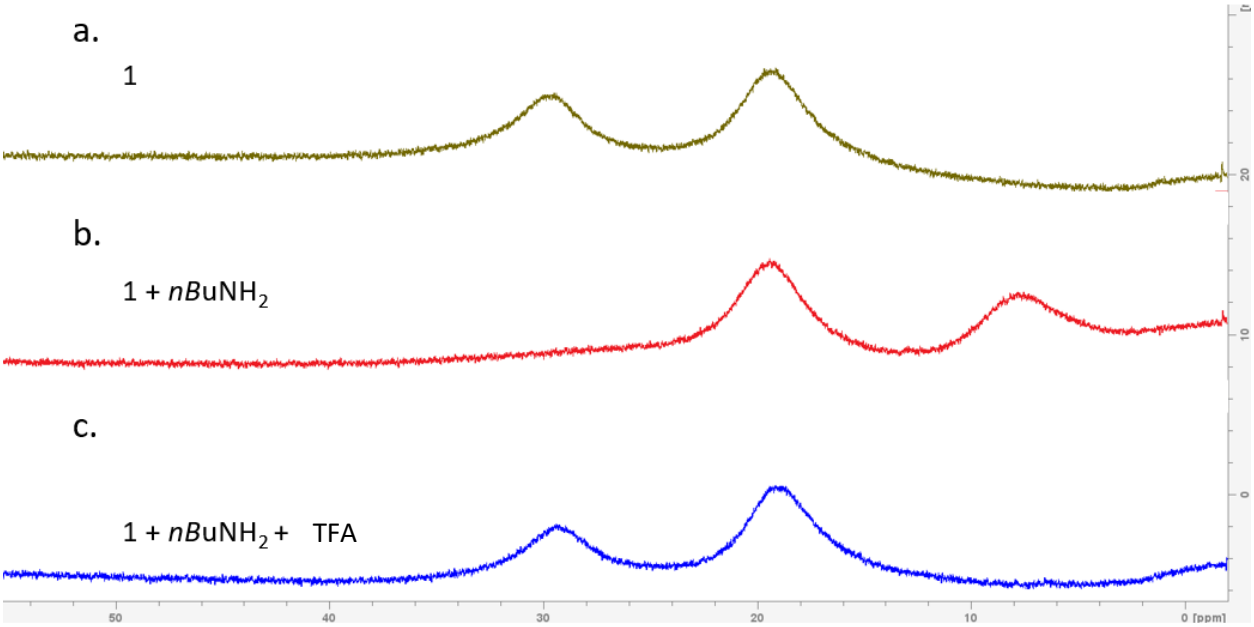

Fig. S5. ^{11}B NMR spectra of **1** using an isolated internal reference standard of boric acid (19.3 ppm). (a) Free **1** in $CDCl_3$ (29.6 ppm). (b) **1** with two equivalents of *n*$BuNH_2$ in $CDCl_3$. This interaction shifts the ^{11}B resonance to 7.6 ppm. (c) **1** with two equivalents of *n*$BuNH_2$ and excess of TFA in $CDCl_3$, the TFA protonates the amine, releasing them from **1** and regenerating the peak at 29.6 ppm for free host **1**.

Synthesis and Characterization

3-Methoxycatechol was obtained according to a literature procedure.[3] Chemicals for all the synthesis purchased from Acros and Sigma-Aldrich were used without further purification. All solvents were obtained from purification systems from Innovative Technologies.

Compound **1**: To a mixture of 2,5-thiophenediboronic (350 mg, 2 mmol) and catechol (529 mg, 4.8 mmol) 50 ml of dry toluene was added in a flask. The solution was heated to 140 ºC to reflux under a nitrogen atmosphere with Dean-Stark trap. After refluxed overnight, clear solution was cooled to room temperature and solvent was removed by rotary evaporation. The excess catechol was removed by a Kugel-Rohr at 95-100 ºC under reduced pressure for 5 hours. White powder (270 mg, 84%) was obtained. ^{1}H NMR (300 MHz, $CDCl_3$): δ 8.08 (s, 2H), 7.34 (m, 4H), 7.16 (m, 4H); ^{13}C NMR (100 MHz, $CDCl_3$): δ 148.2, 139.5, 123.1, 112.7, 105.0; ^{11}B NMR (128.42 MHz, $CDCl_3$, $BF_3 \cdot Et_2O$= 0 ppm as the external reference and boric acid as the second reference at 19.3 ppm): δ 29.6; HR-MS: found, m/z 320.0493; calcd for $C_{16}H_{10}B_2O_4S$: 320.0492. White crystal of **1** was obtained from a slow evaporation method of benzene. White crystal of **1**-2F was obtained from a slow diffusion method of a mixture of compound **1** (20 mM) and two equivalent of tetra-*n*-butylammonium fluoride (TBAF) in $CDCl_3$.

Compound **2**: A mixture of 2,5-thiophenediboronic (50.2 mg, 0.29 mmol) and ethyl-3,4-dihydroxybenzoate (106.2 mg, 0.58 mmol) was refluxed in 30 mL toluene. White powder was obtained as final product (85.6 mg, 65.9%). ^{1}H NMR (300 MHz, $CDCl_3$): δ 8.11 (s, 2H), 8.02 (d, J = 1.5 Hz, 2H), 7.97 (q, 2H), 7.37 (d, J = 8.1 Hz, 2H), 4.41 (q, 4H), 1.02 (t, 12H); ^{13}C NMR (100 MHz, $CDCl_3$): δ 166.0, 151.8, 148.0, 140.0, 126.0, 125.8,114.0, 112.3, 61.2, 14.3; HR-MS: found, m/z 464.0912; calcd for $C_{22}H_{18}B_2O_8S$: 464.0917.

Compound **3**: A mixture of 2,5-thiophenediboronic (68.9 mg, 0.40 mmol) and 4-methoxycatechol (123.6 mg, 0.88 mmol) was refluxed in 30 mL toluene. Gray powder was obtained as final product (141.8 mg, 93.3%). ^{1}H NMR (300 MHz, $CDCl_3$): δ 8.04 (s, 2H), 7.21 (d, J = 8.7 Hz, 4H), 6.94 (d, J = 2.4 Hz, 4H); ^{13}C NMR (100 MHz, $CDCl_3$): δ 156.1, 149.1, 142.5, 134.4, 112.1, 108.0, 99.7, 56.1; HR-MS: found, m/z 380.0712; calcd for $C_{18}H_{14}B_2O_6S$: 380.0704.

Compound **4**: A mixture of 2,5-thiophenediboronic (50.0 mg, 0.29 mmol) and 3,5-di-tert-butylcatechol (142.4 mg, 0.64 mmol) was refluxed in 50 mL toluene overnight. White powder was obtained as final product (111 mg, 70%).^{1}H NMR (300 MHz, CD_2Cl_2): δ 8.08 (s, 2H), 7.26 (d, J= 1.2 Hz, 2H), 7.14 (d, J = 1.5 Hz, 2H), 1.52 (s, 18H), 1.36 (s, 18H); ^{13}C NMR (100 MHz, $CDCl_3$): δ 148.1, 146.1, 143.8, 139.0, 135.1, 116.8, 107.7, 35.0, 34.5, 31.9, 31.8, 29.8; HR-MS: found, m/z 544.3000 ; calcd for $C_{32}H_{42}B_2O_4S$: 544.3001.

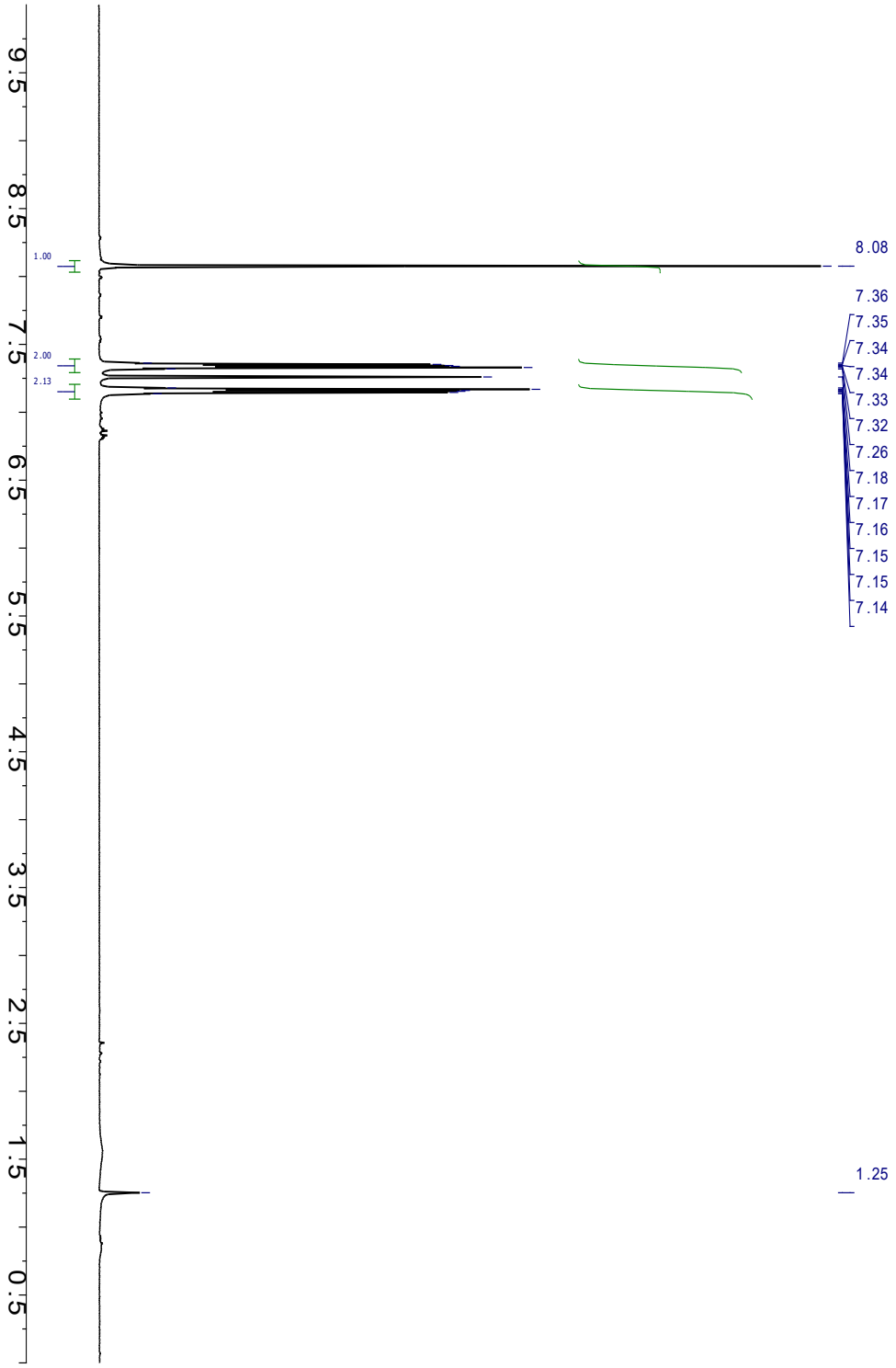

Fig. S6. ^{1}H NMR of Bis(dioxaborole) **1.**

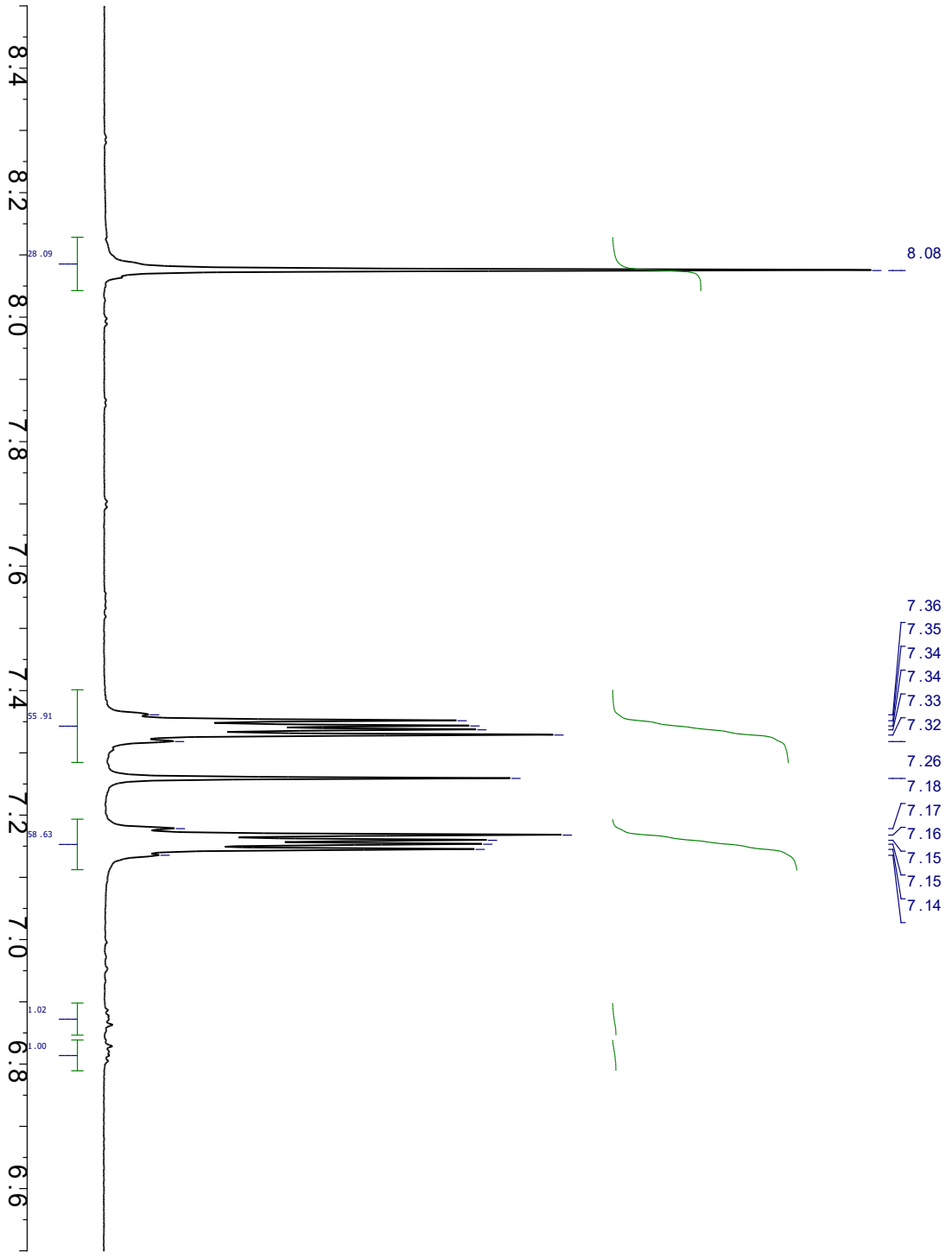

Fig. S7. ^{1}H NMR of Compound **1** – blow-up from 6.5-8.5 ppm.

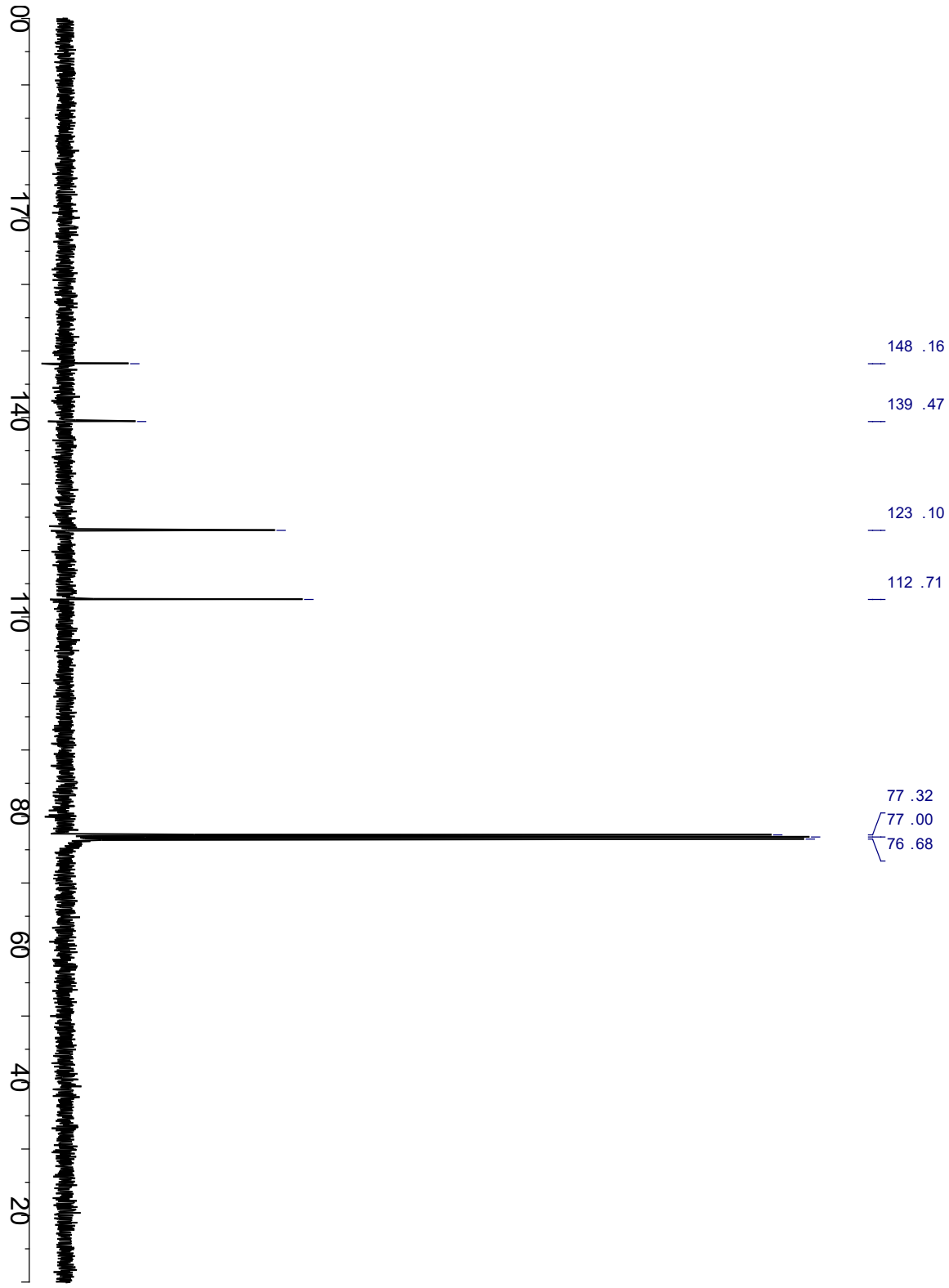

Fig. S8. ^{13}C NMR of Compound **1.**

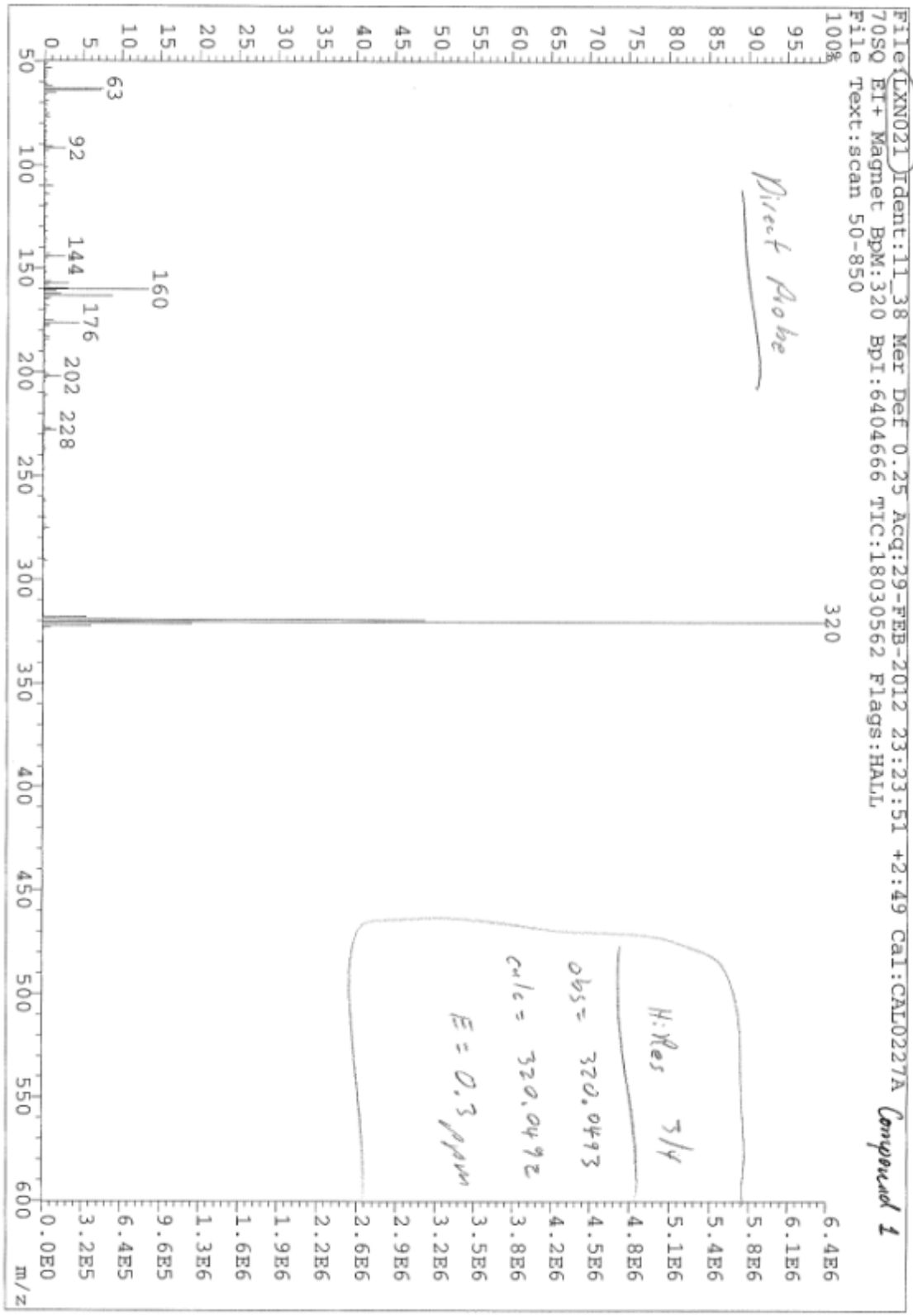

Fig. S9. HRMS of Compound **1.**

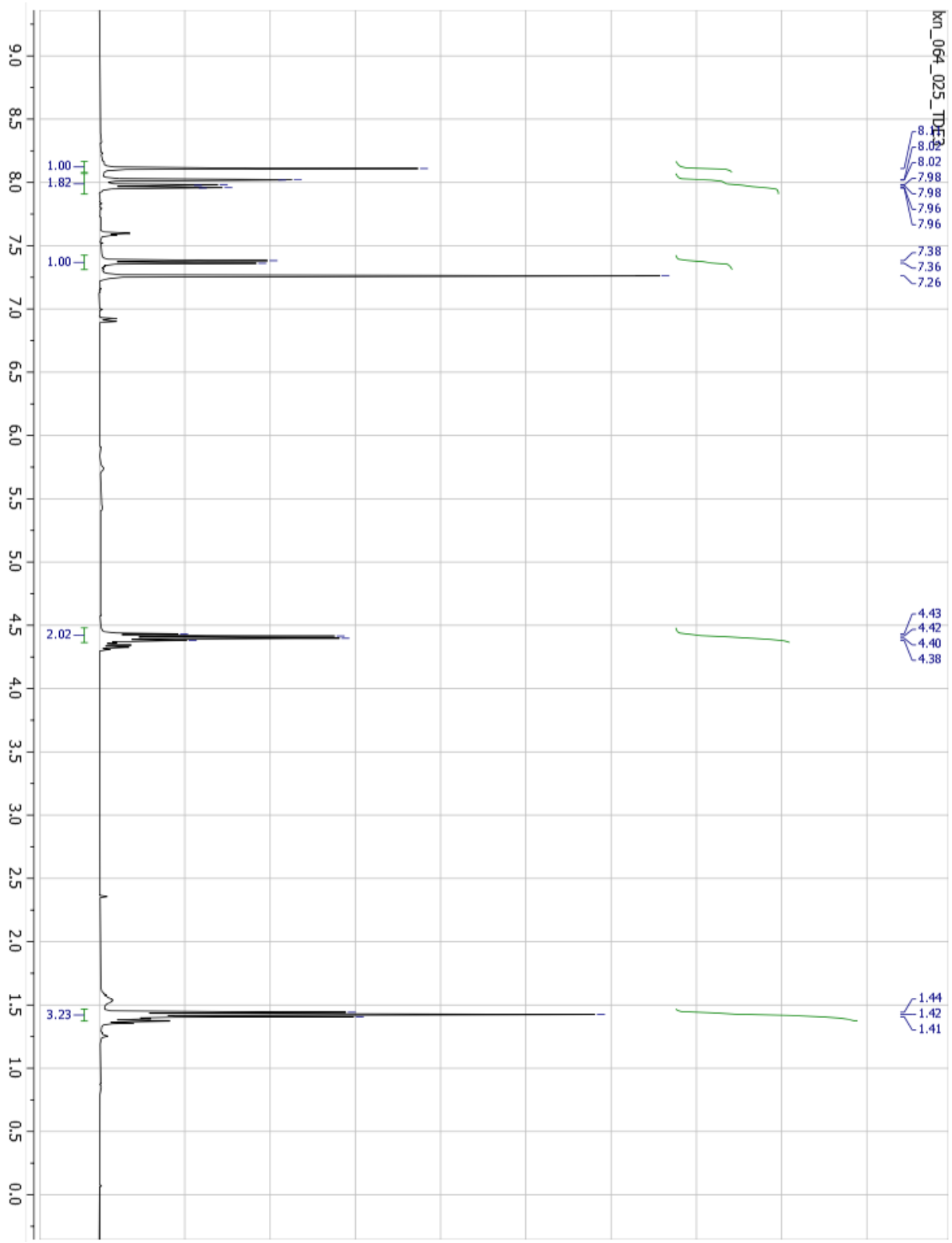

Fig. S10. ^{1}H NMR of Compound **2.**

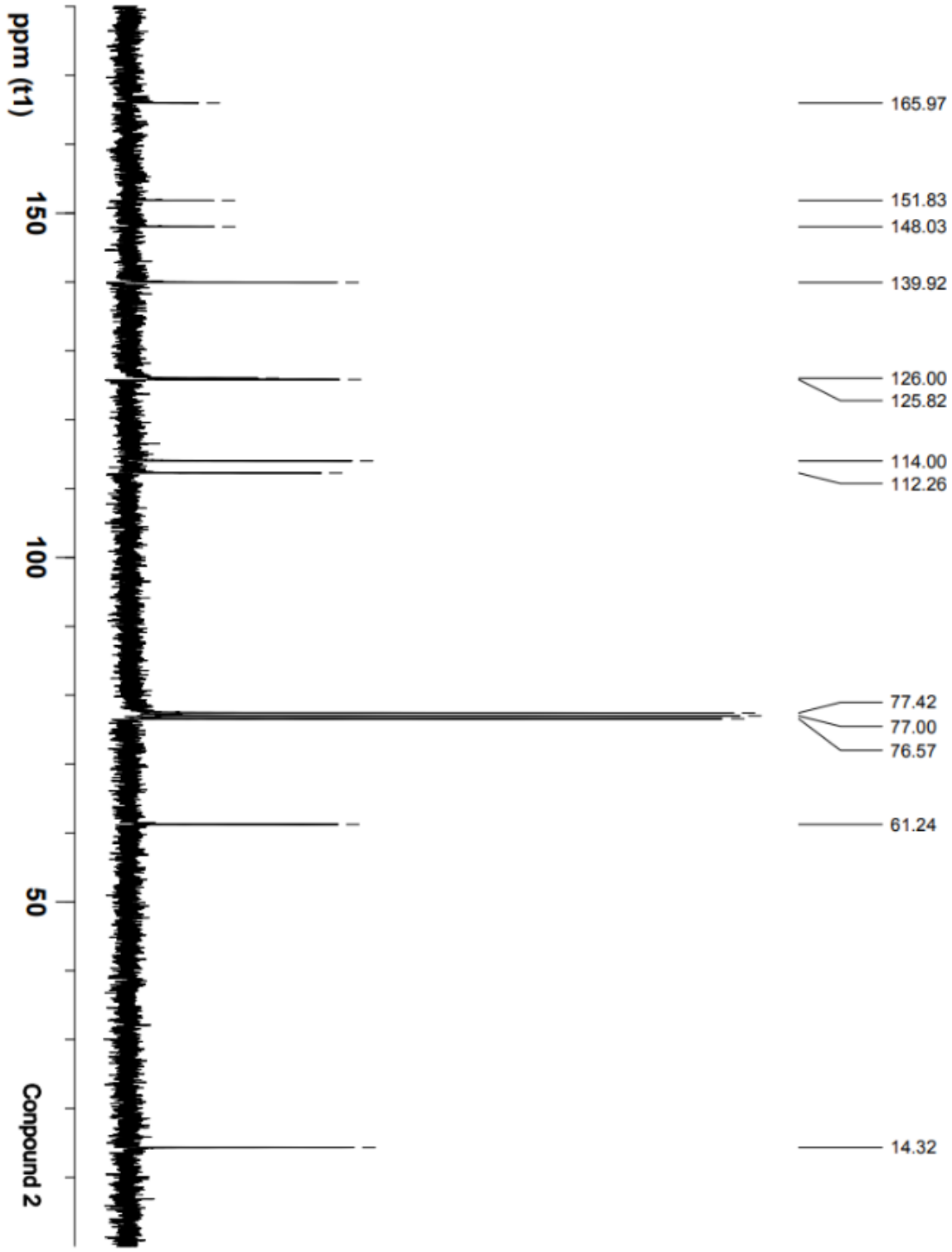

Fig. S11. ^{13}C NMR of Compound **2.**

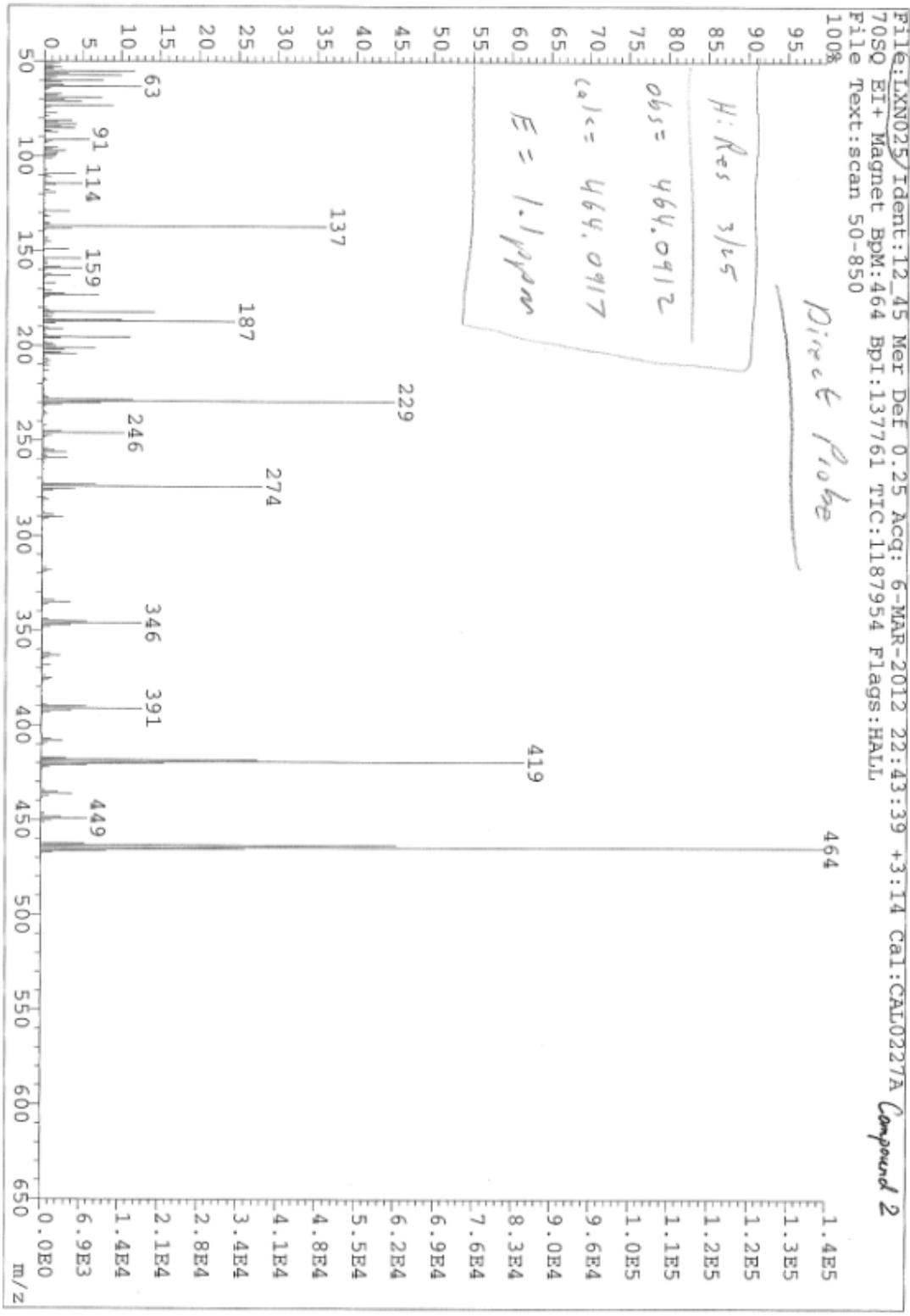

Fig. S12. HR-MS of Compound **2.**

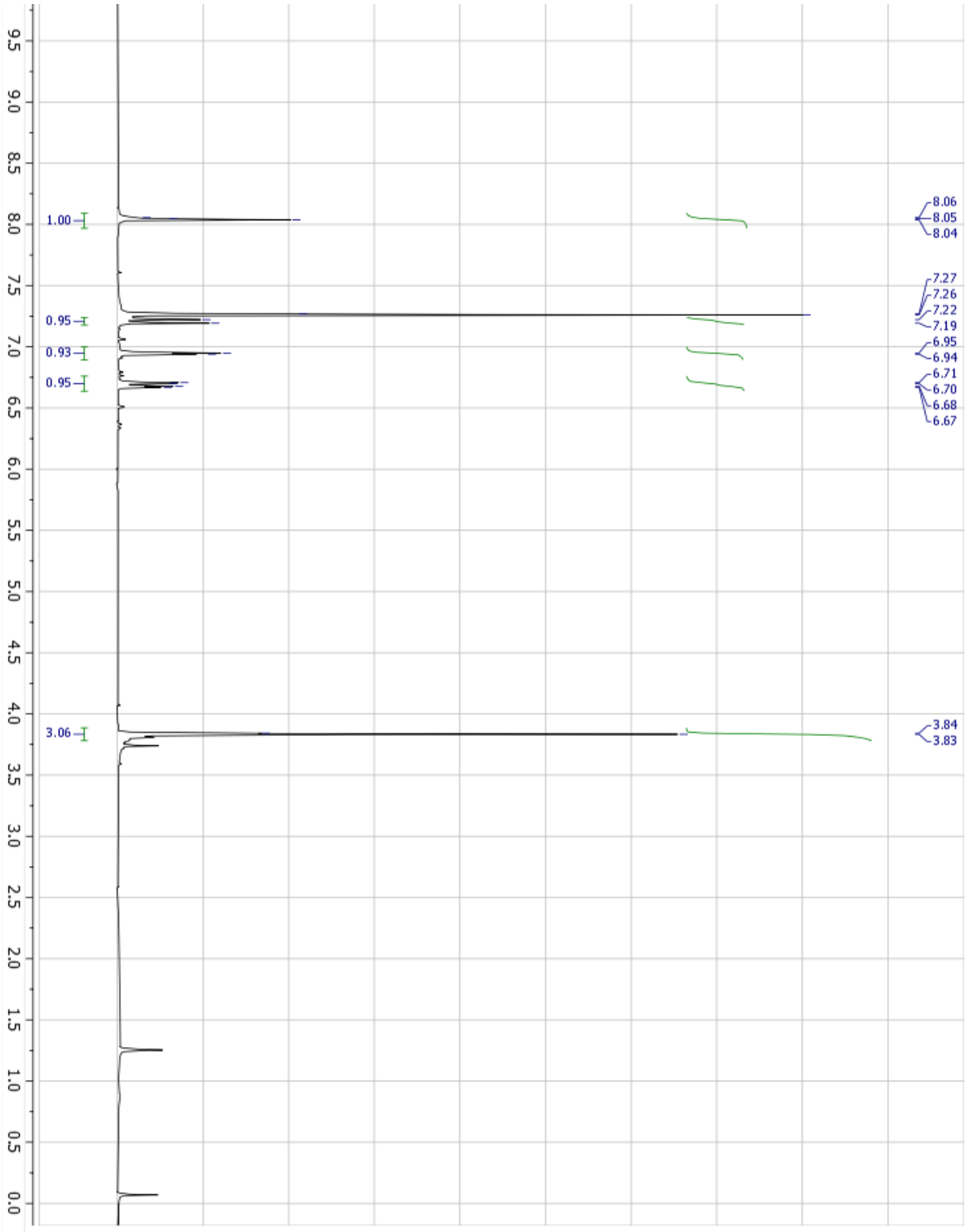

Fig. S13. ^{1}H NMR of Compound **3.**

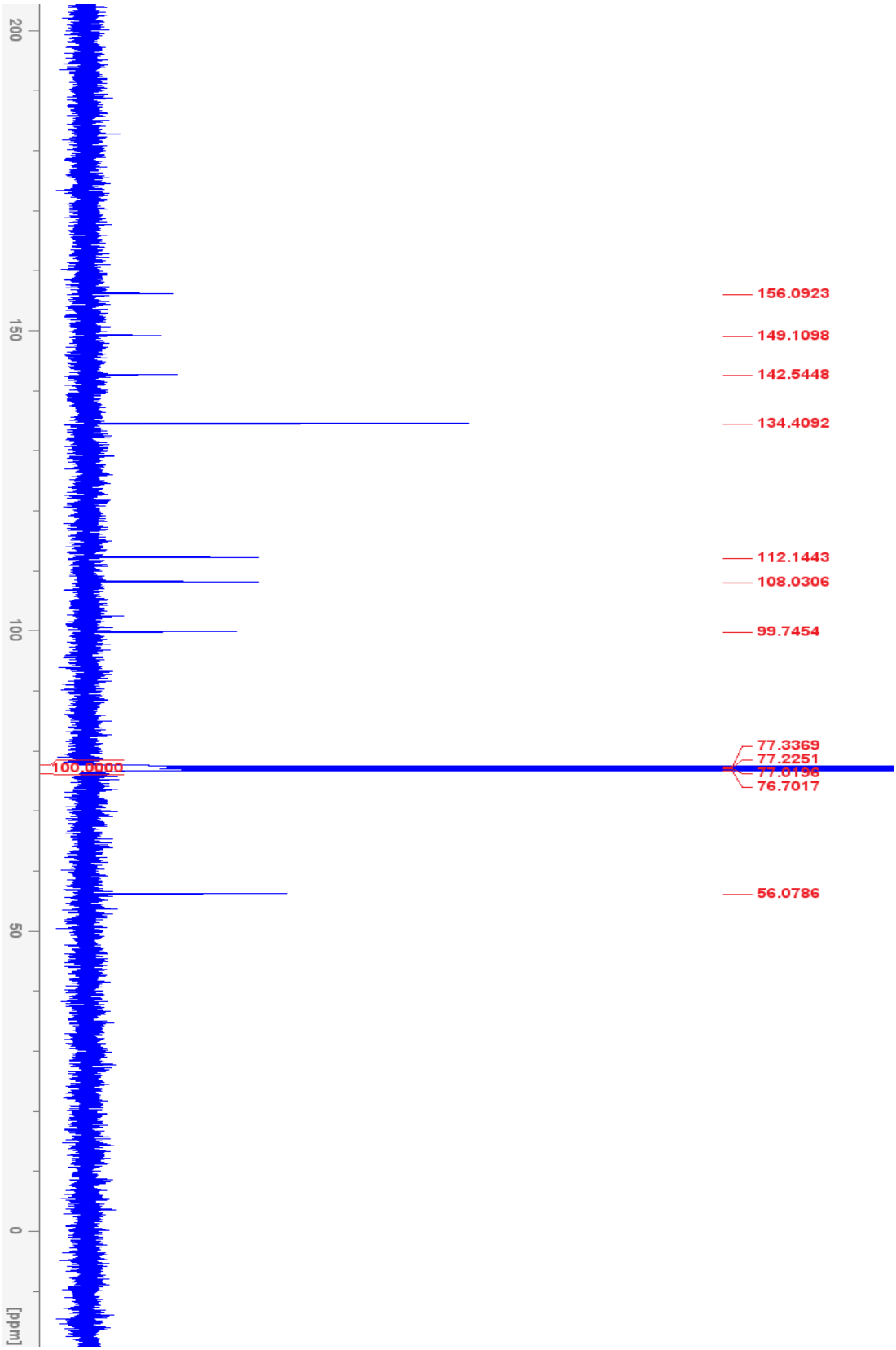

Fig. S14. ^{13}C NMR of Compound **3.**

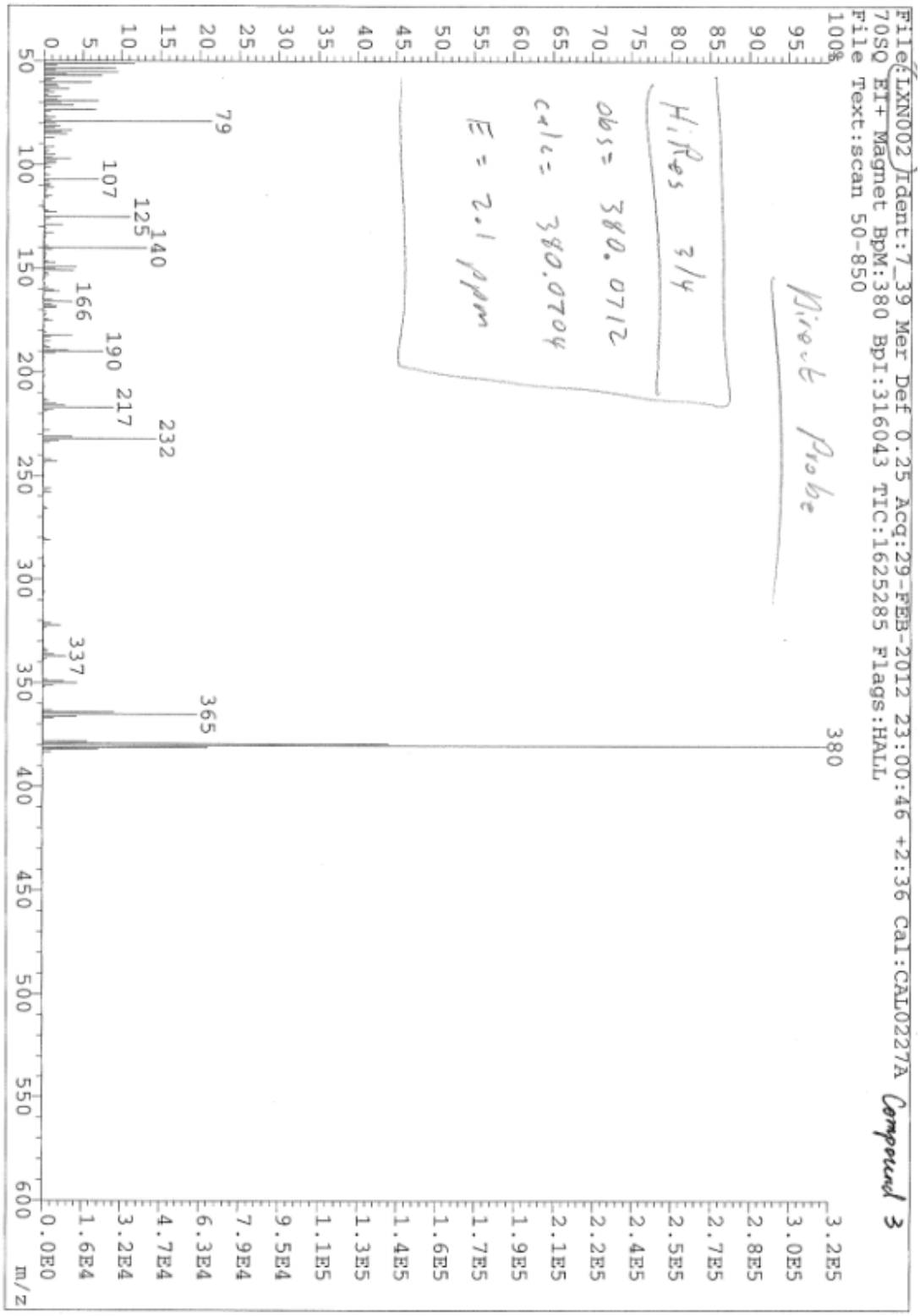

Fig. S15. HR-MS of Compound **3.**

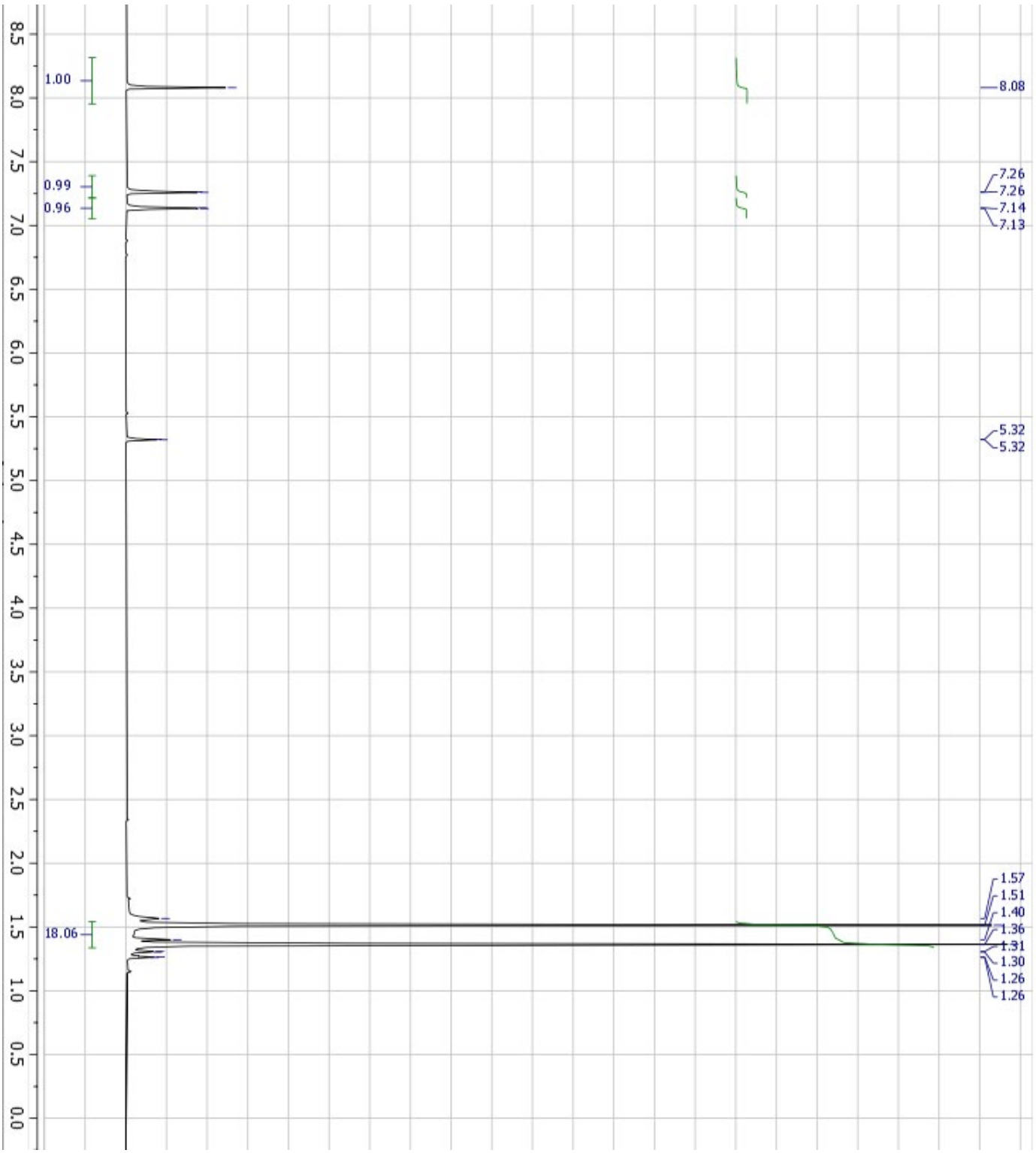

Fig. S16. ^{1}H NMR of Compound **4.**

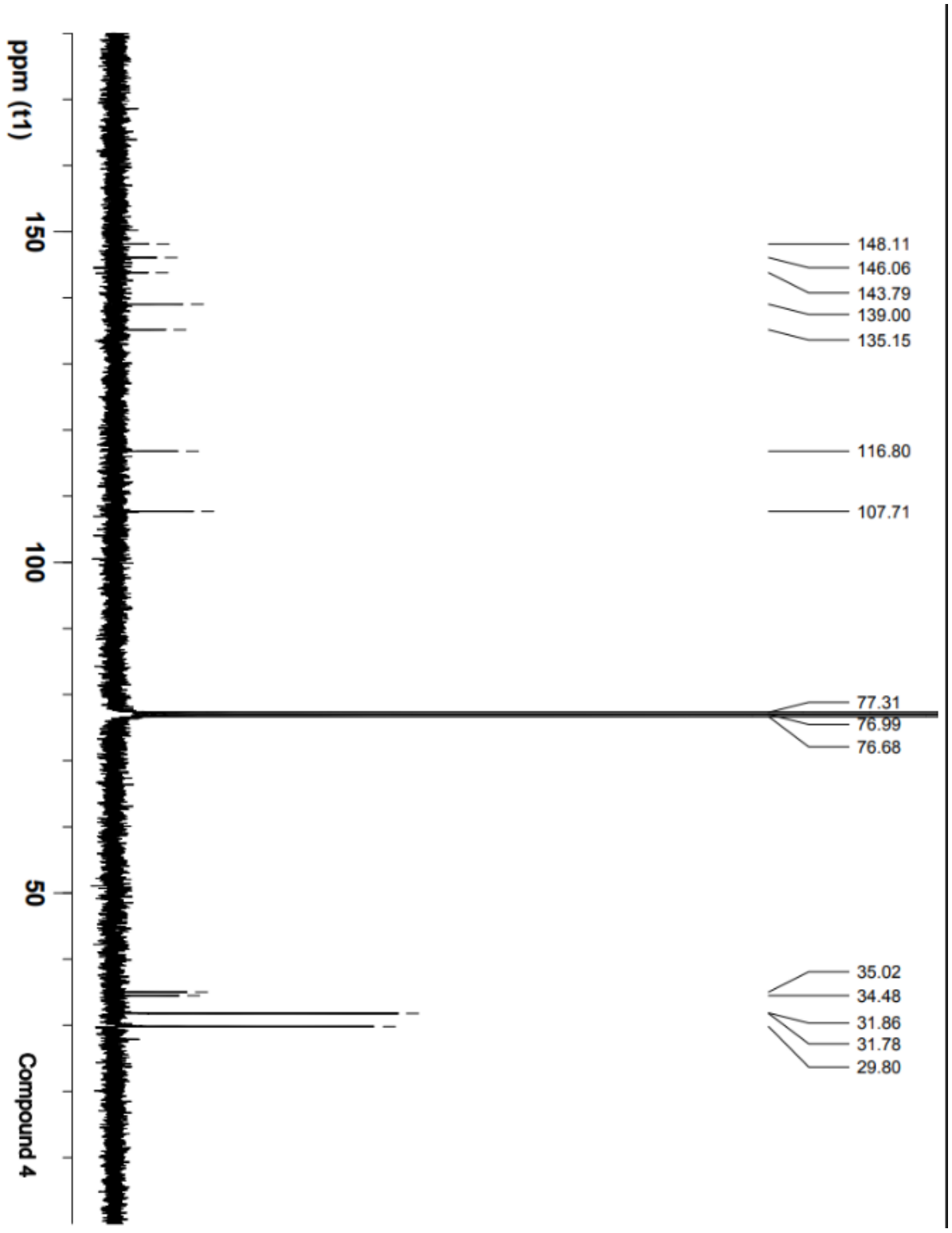

Fig. S17. ^{13}C NMR of Compound **4.**

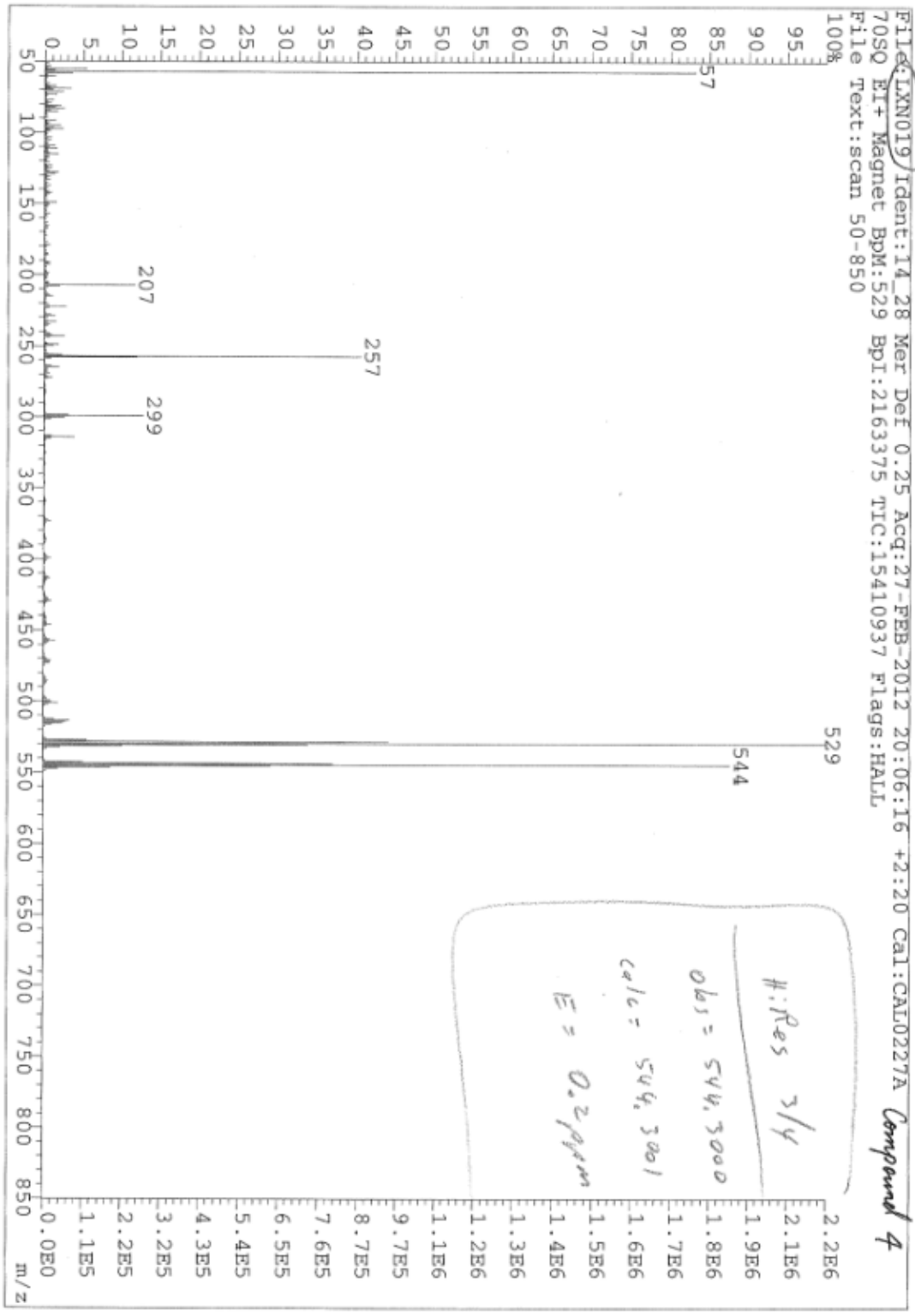

Fig. S18. HR-MS of Compound **4.**

Absorption Titration Spectra and Data Fitting

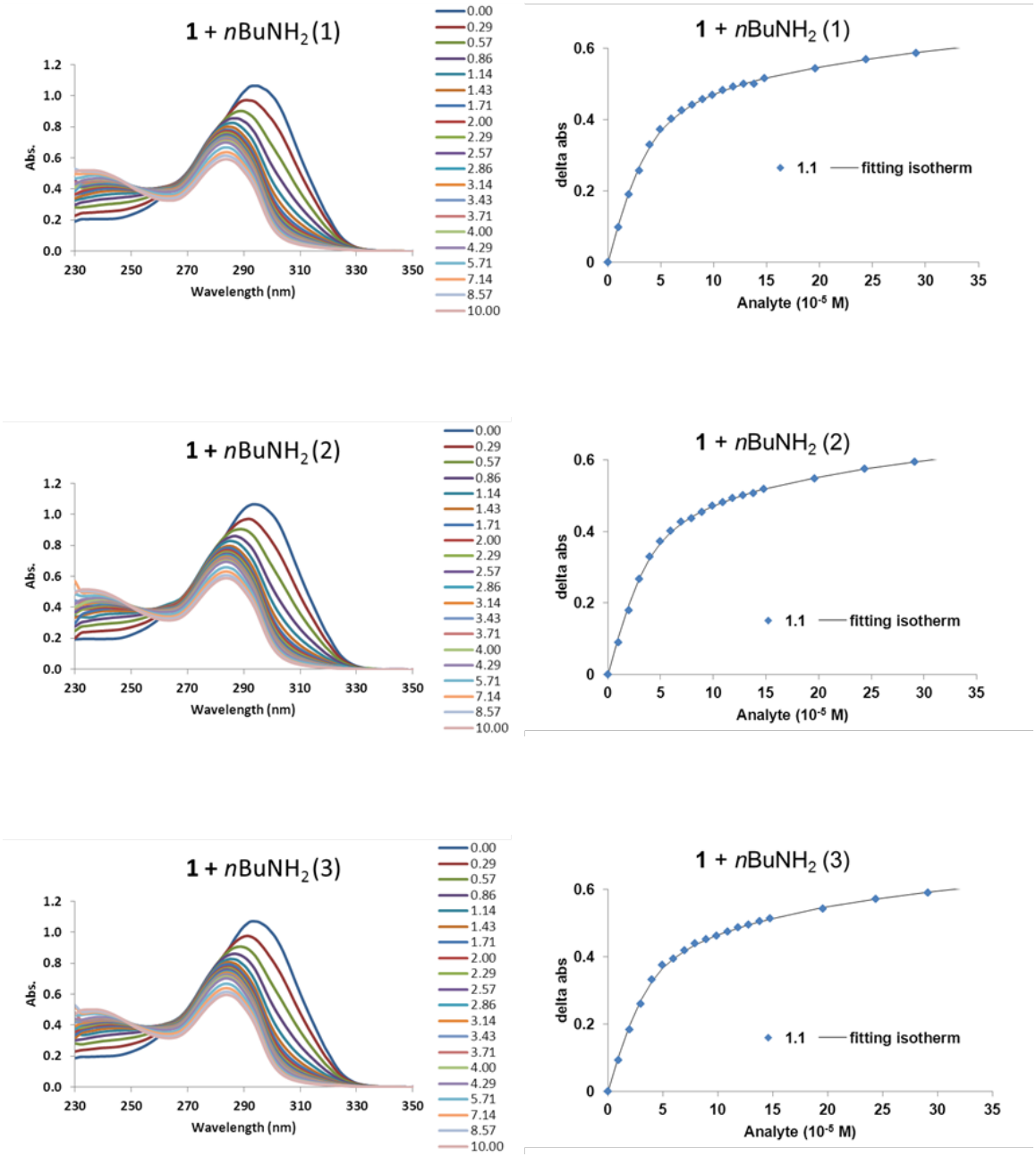

Fig. S19. Absorption titration curves and binding isotherms of compound **1** with *n*BuNH$_2$.

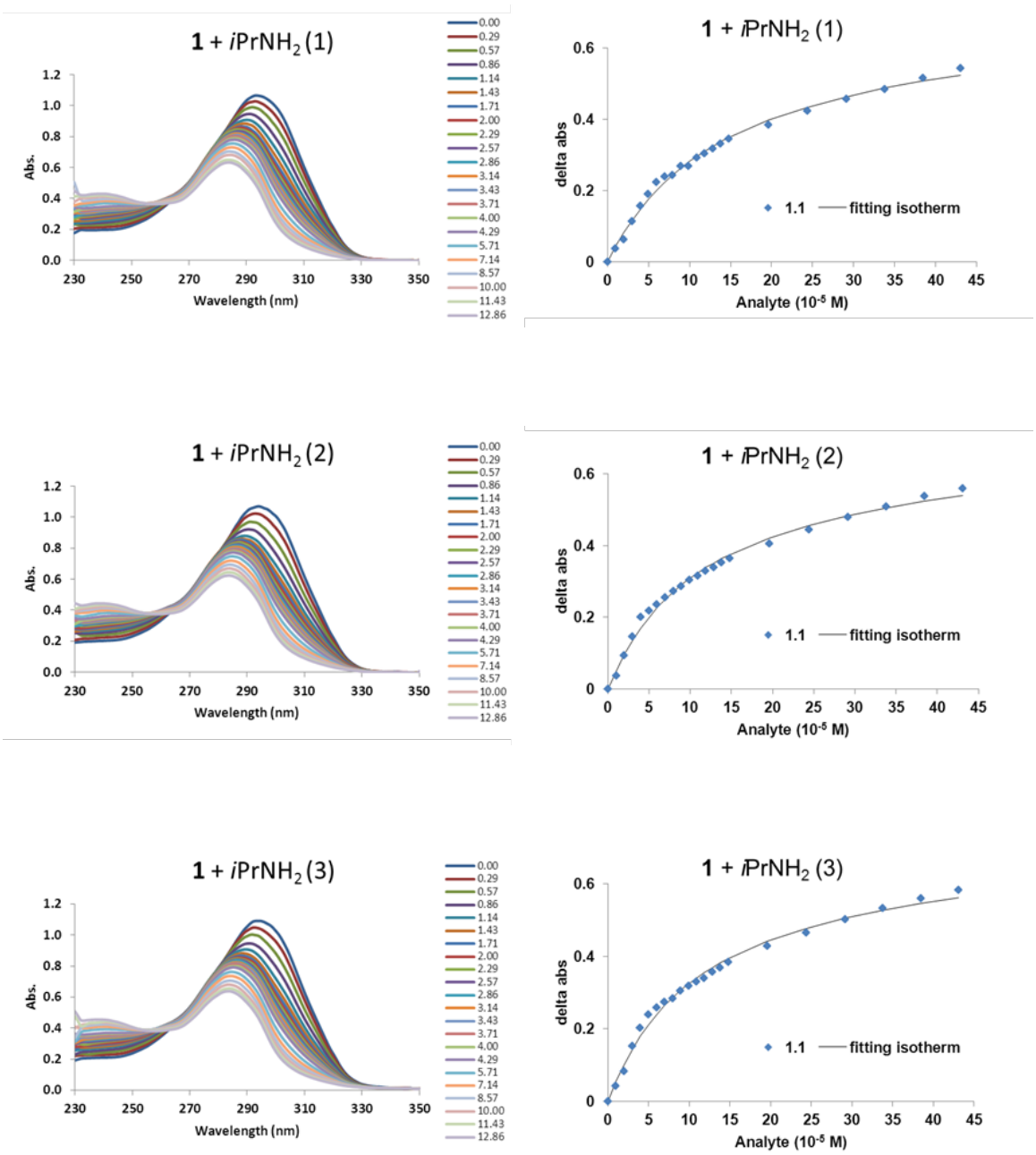

Fig. S20. Absorption titration curves and binding isotherms of compound **1** with *i*PrNH$_2$.

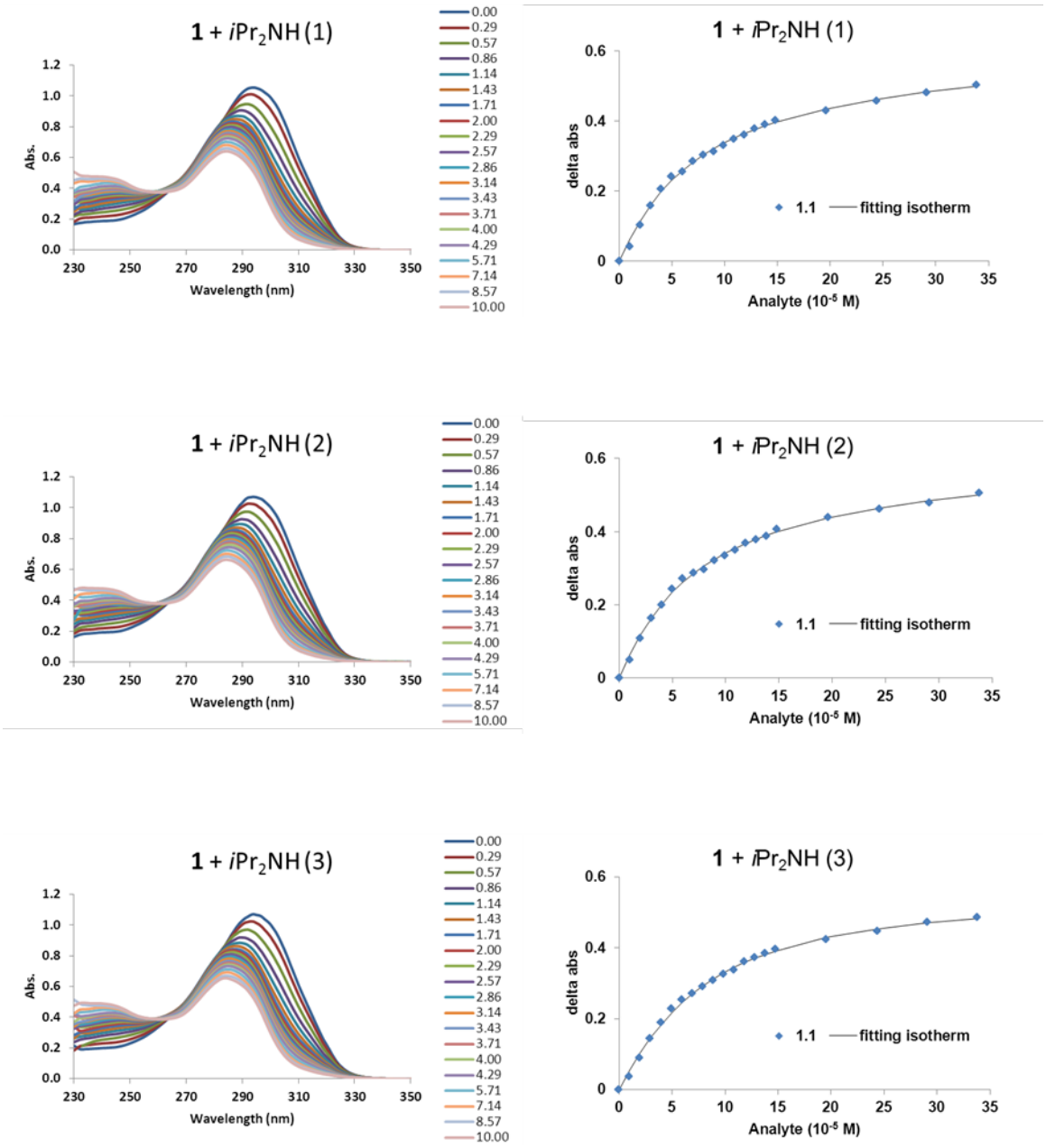

Fig. S21. Absorption titration curves and binding isotherms of compound **1** with *i*Pr$_2$NH.

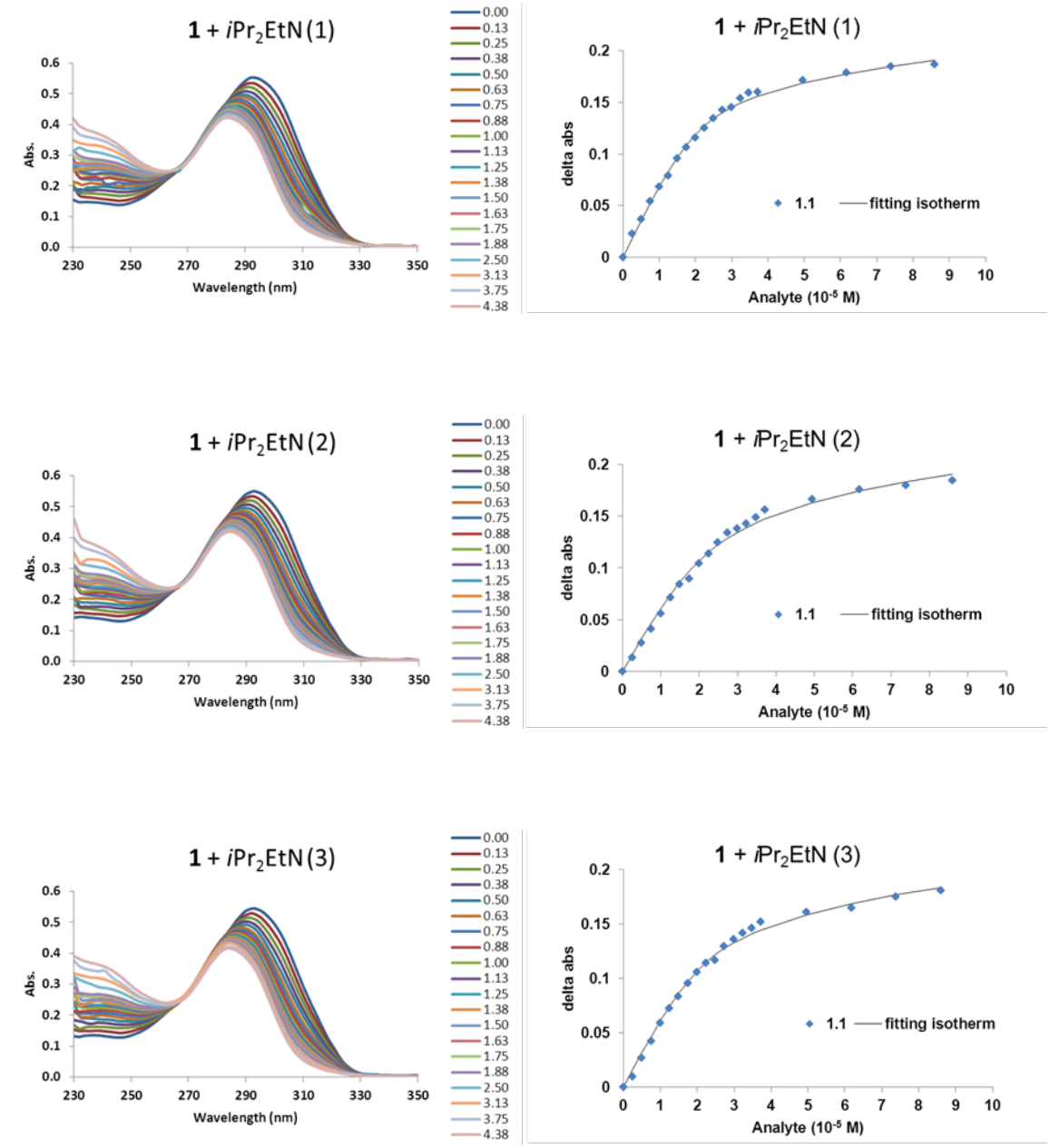

Fig. S22. Absorption titration curves and binding isotherms of compound **1** with *i*Pr$_2$EtN.

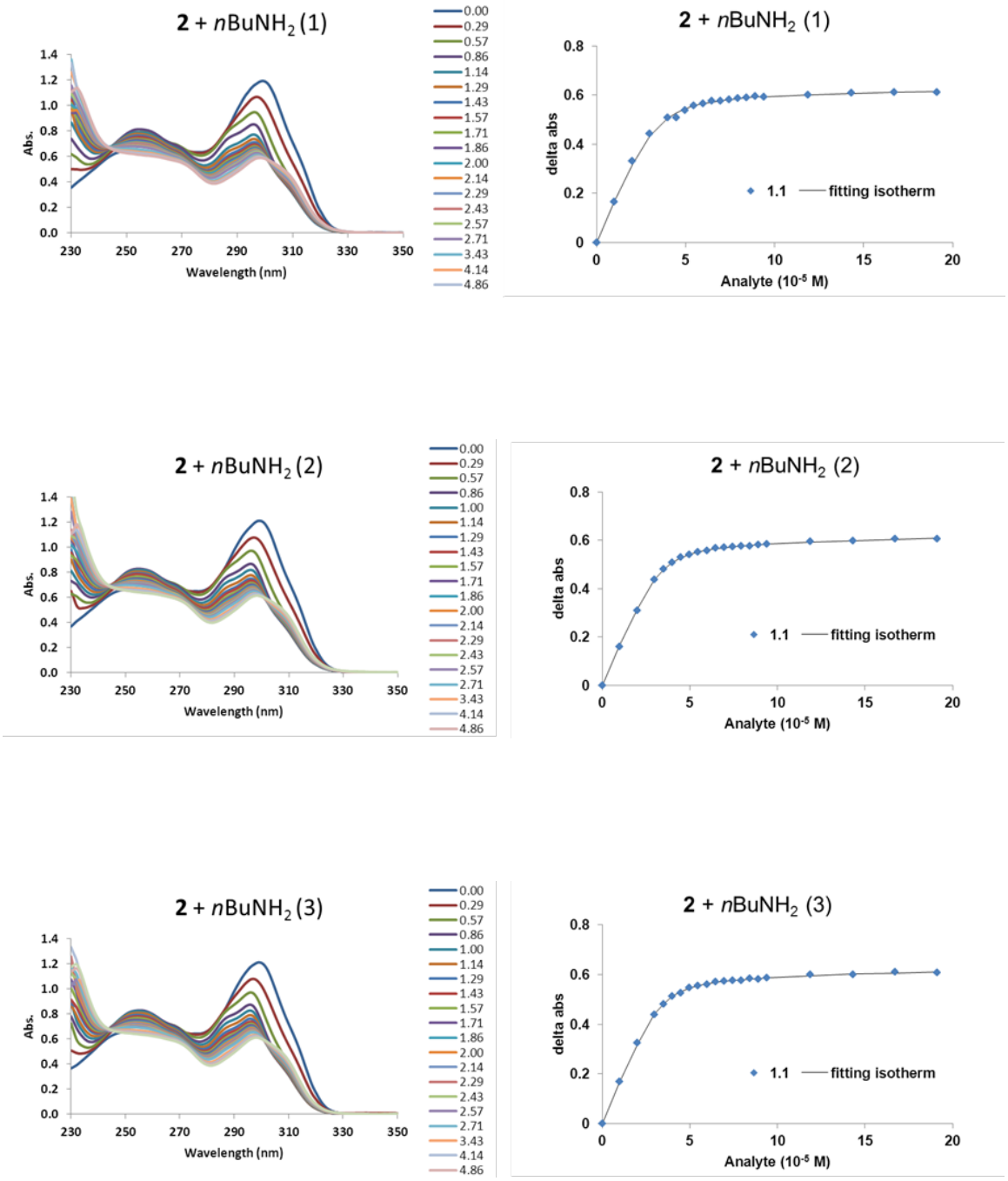

Fig. S23. Absorption titration curves and binding isotherms of compound **2** with *n*BuNH$_2$.

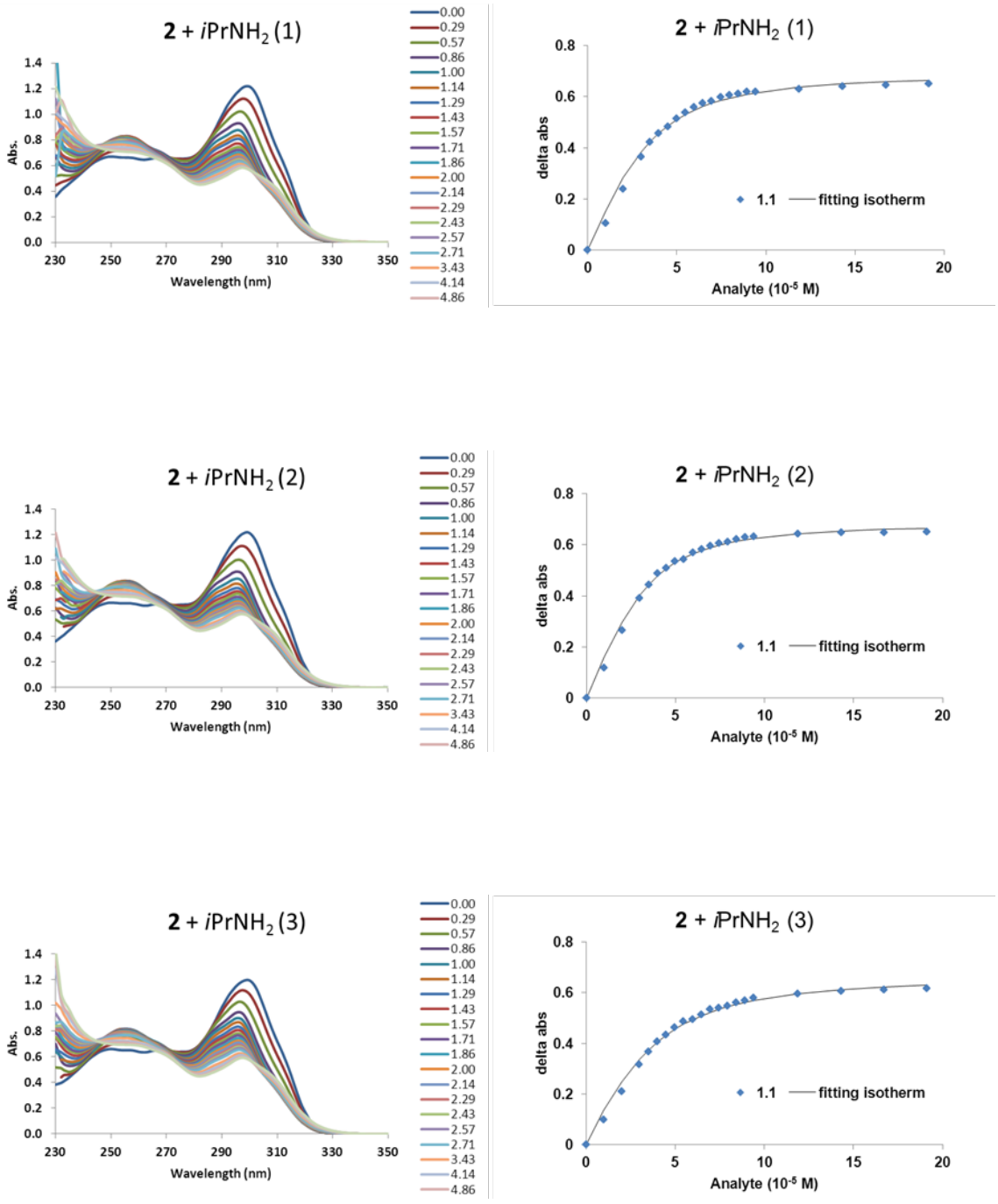

Fig. S24. Absorption titration curves and binding isotherms of compound **2** with *i*PrNH$_2$.

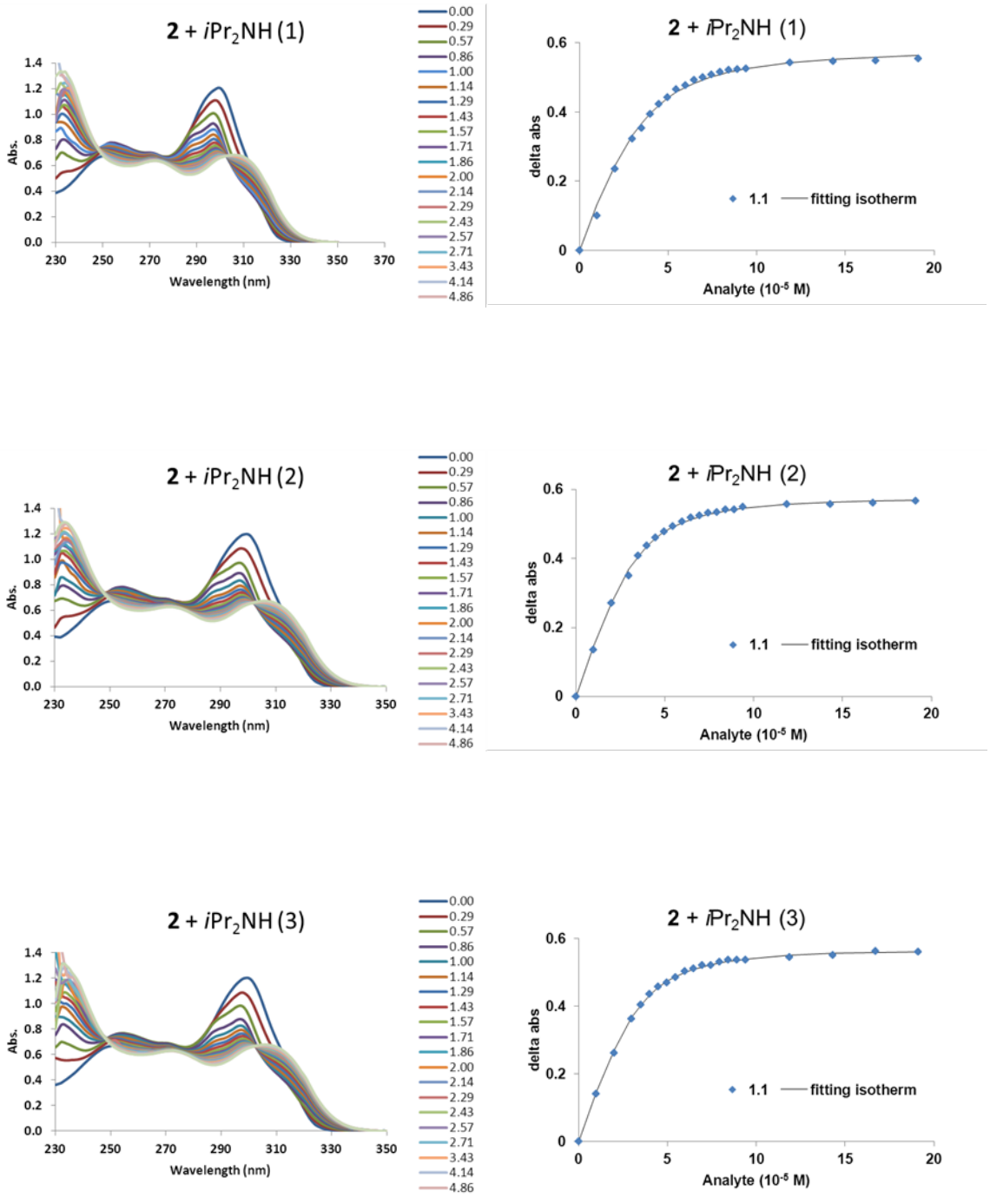

Fig. S25. Absorption titration curves and binding isotherms of compound **2** *i*Pr$_2$NH.

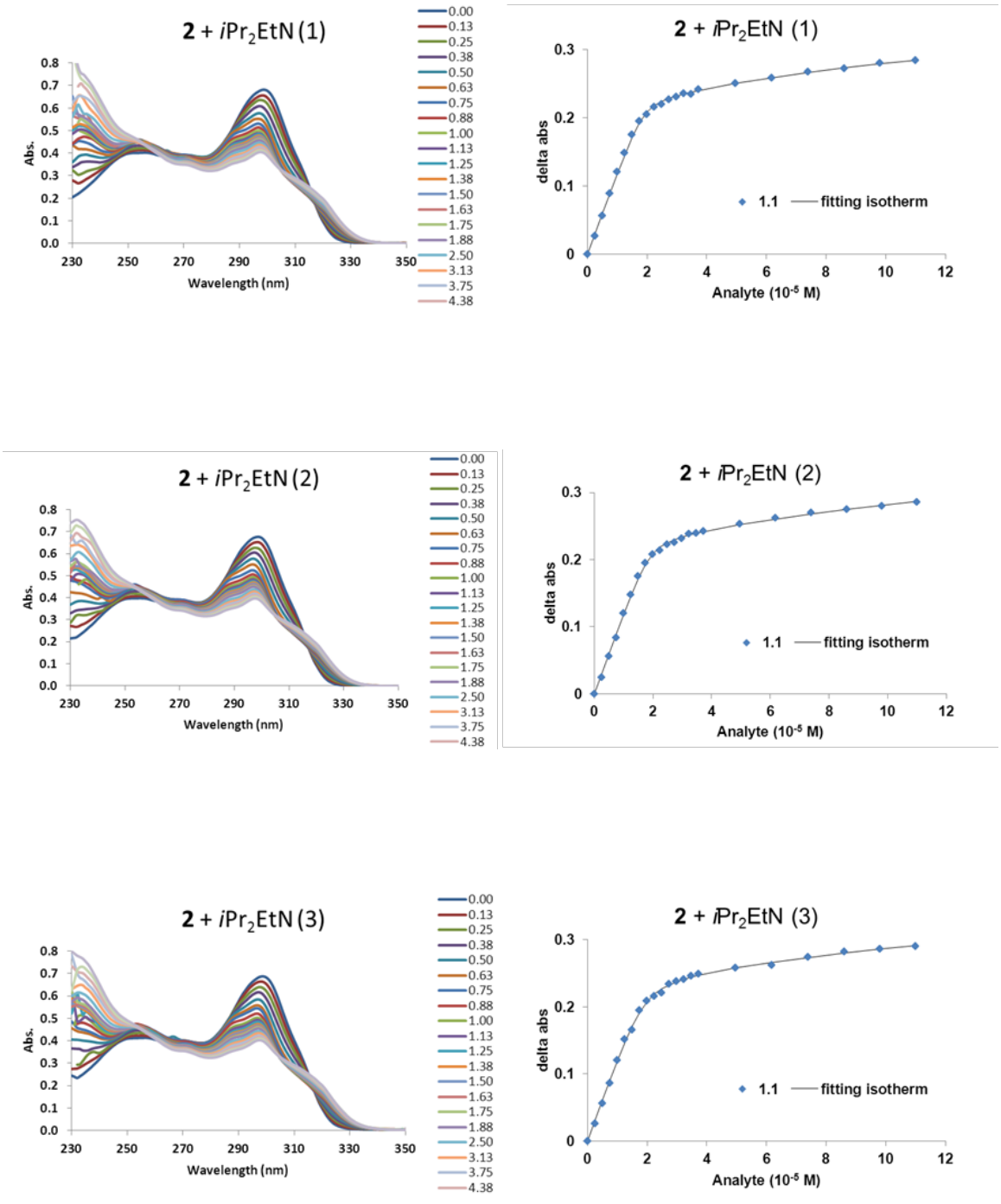

Fig. S26. Absorption titration curves and binding isotherms of compound **2** with *i*Pr$_2$EtN.

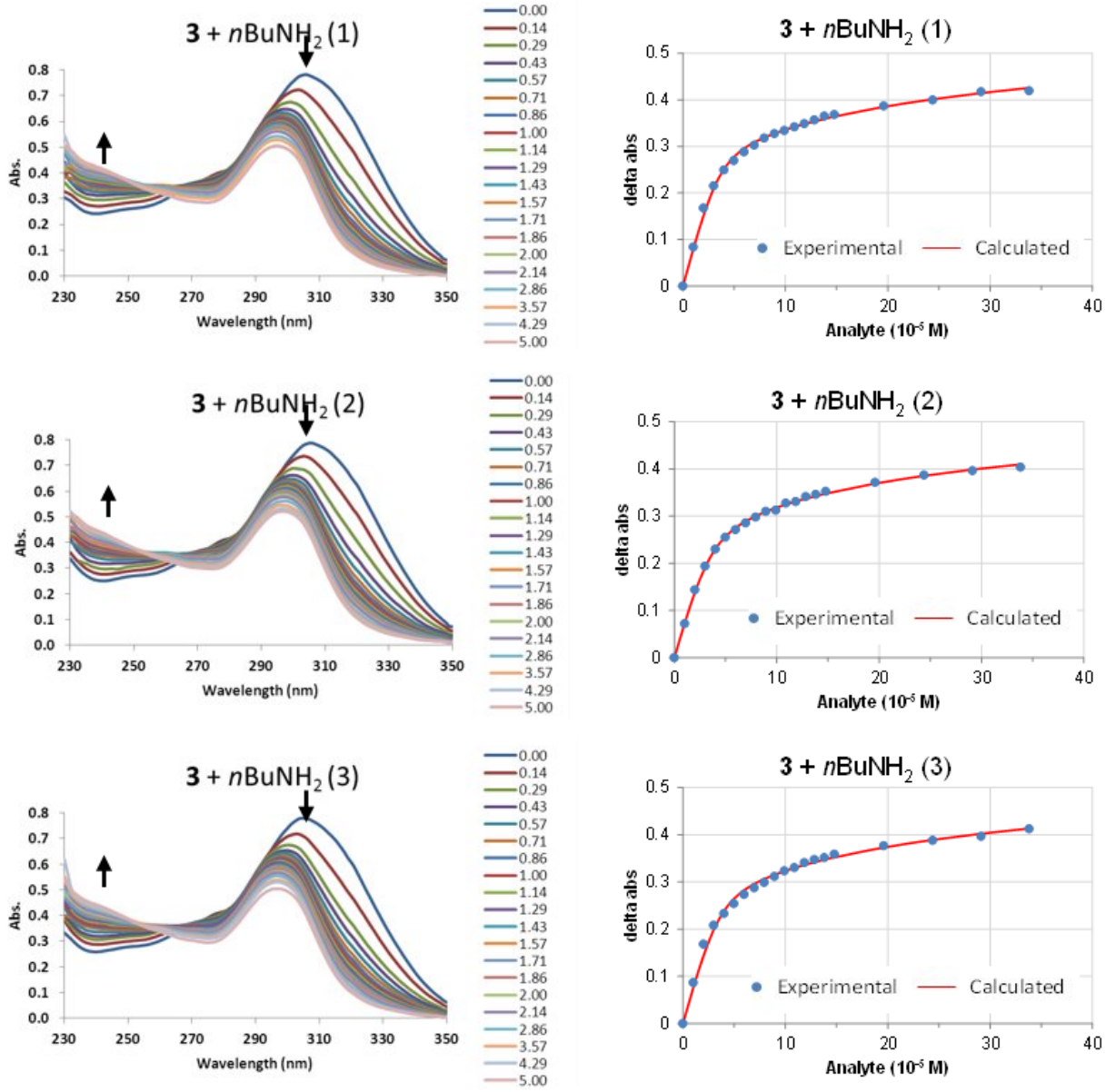

Fig. S27. Absorption titration curves and binding isotherms of compound **3** with *n*BuNH$_2$.

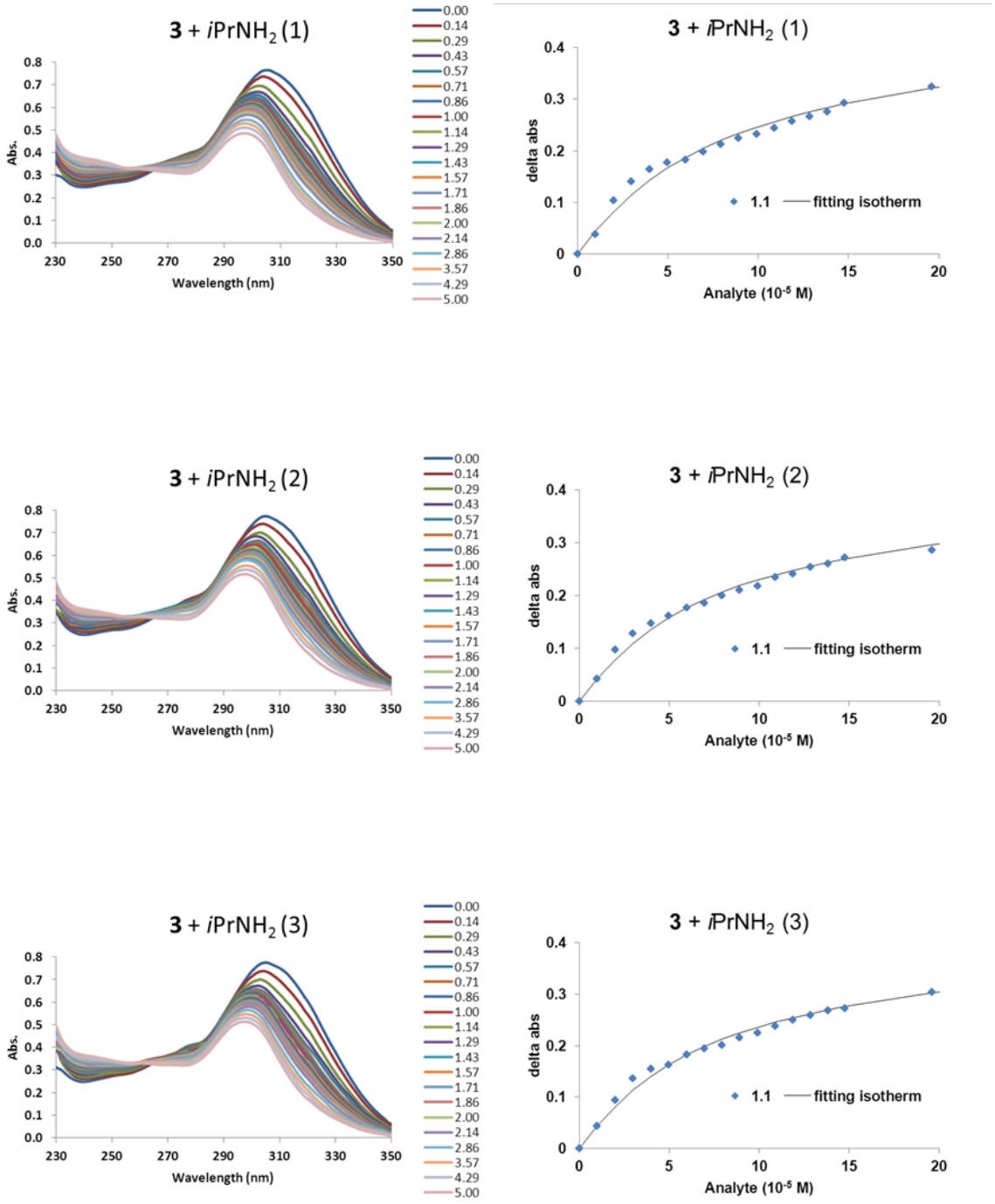

Fig. S28. Absorption titration curves and binding isotherms of compound **3** with *i*PrNH$_2$.

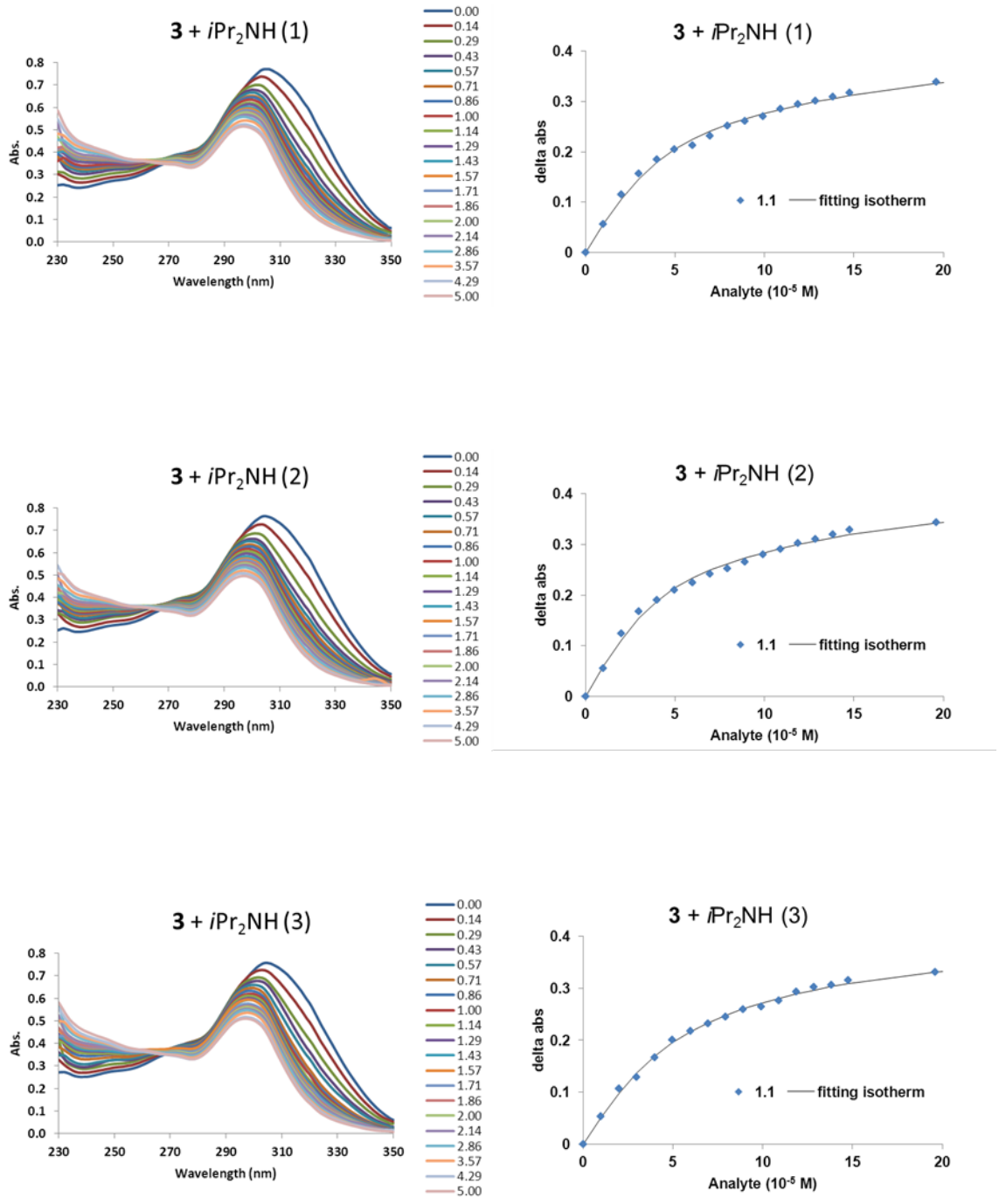

Fig. S29. Absorption titration curves and binding isotherms of compound **3** with *i*Pr$_2$NH.

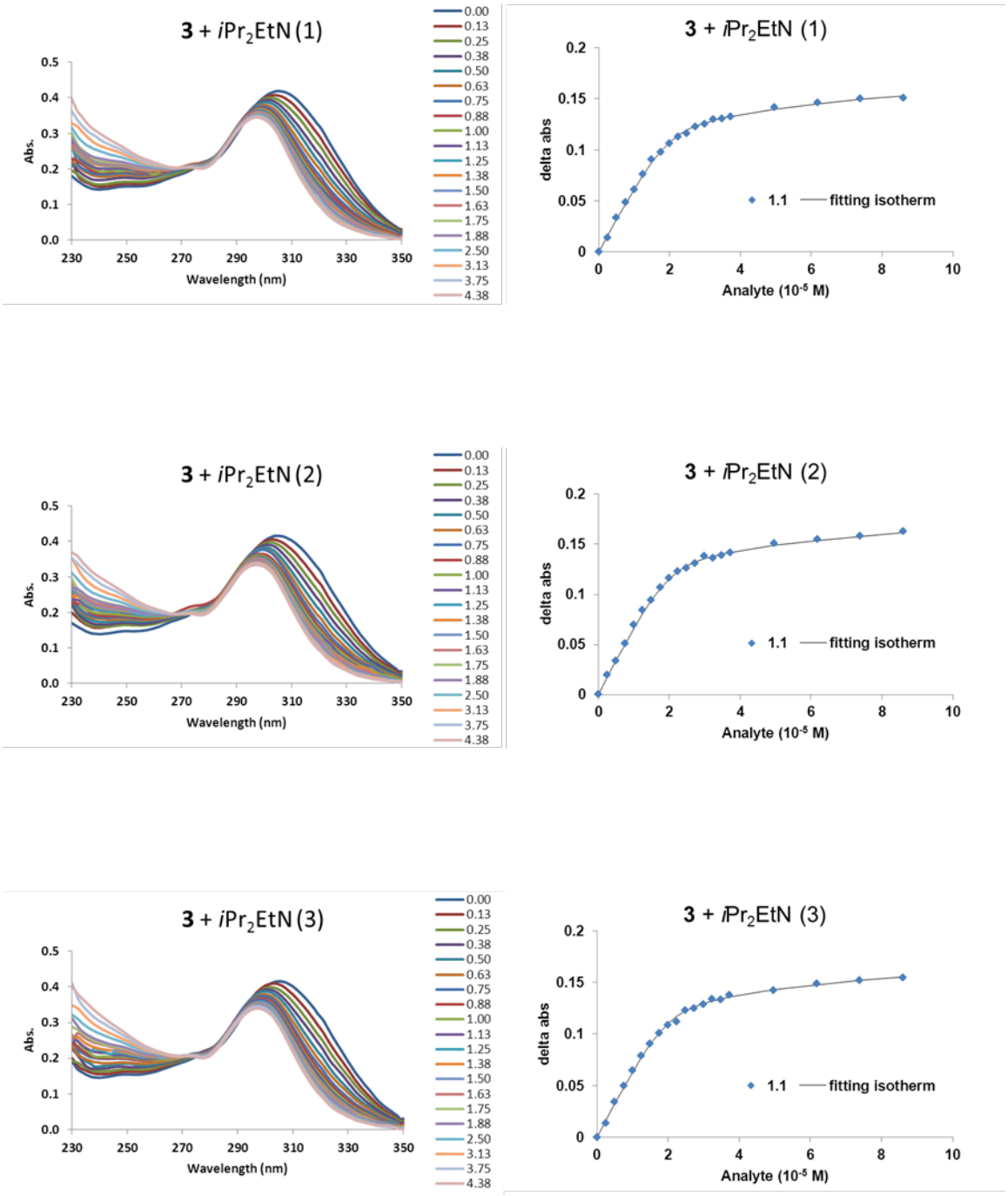

Fig. S30. Absorption titration curves and binding isotherms of compound **3** with *i*Pr$_2$EtN.

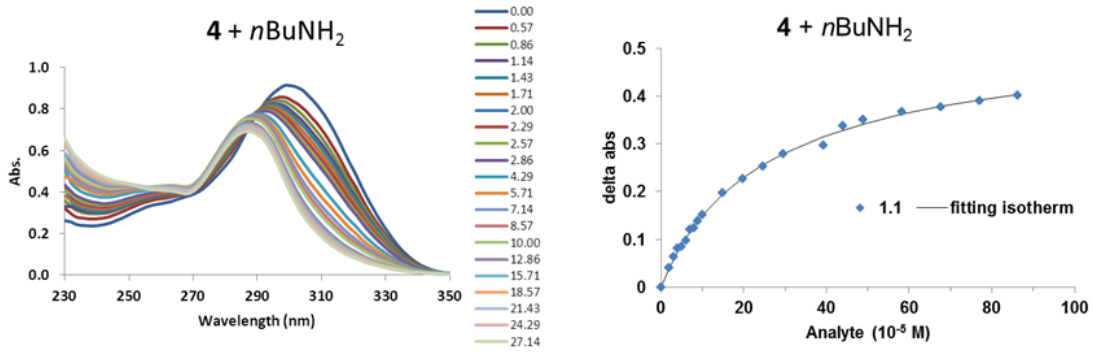

Fig. S31. Absorption titration curves and binding isotherms of compound **4** with nBuNH$_2$.

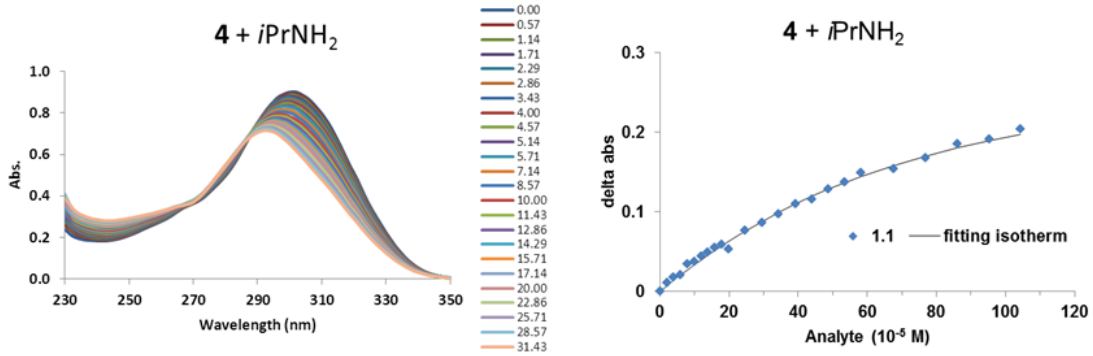

Fig. S32. Absorption titration curves and binding isotherms of compound **4** with iPrNH$_2$.

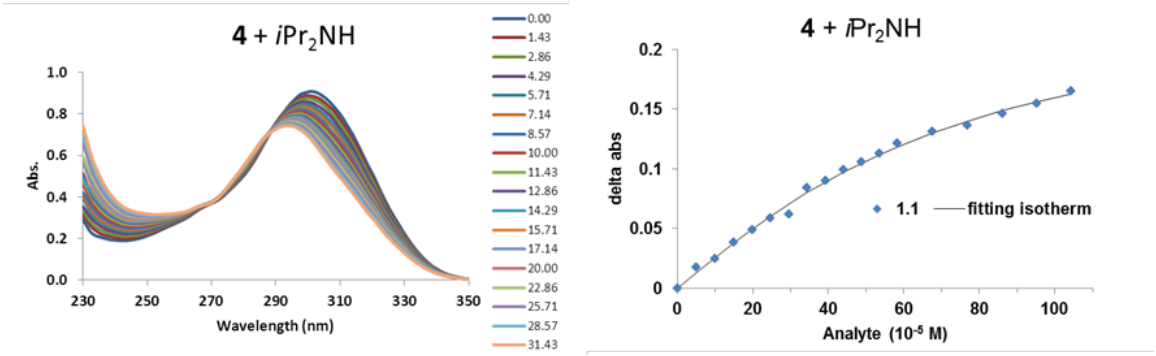

Fig. S33. Absorption titration curves and binding isotherms of compound **4** with iPr$_2$NH.

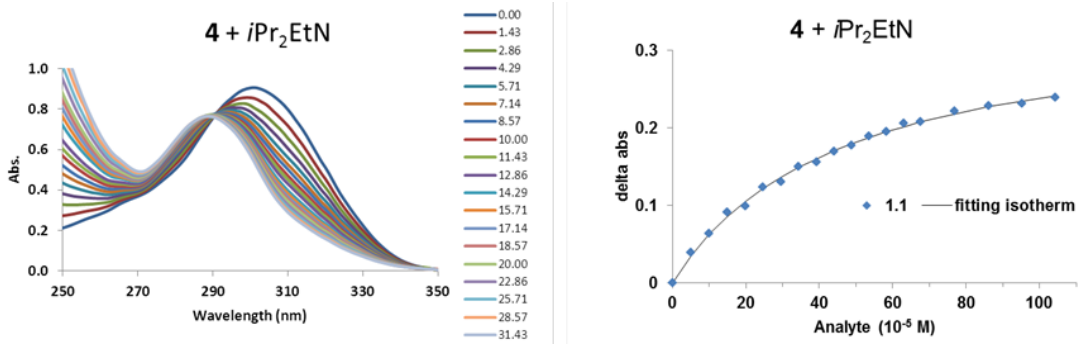

Fig. S34. Absorption titration curves and binding isotherms of compound **4** with *i*Pr$_2$EtN.

Mole Ratio Stoichiometry Plot

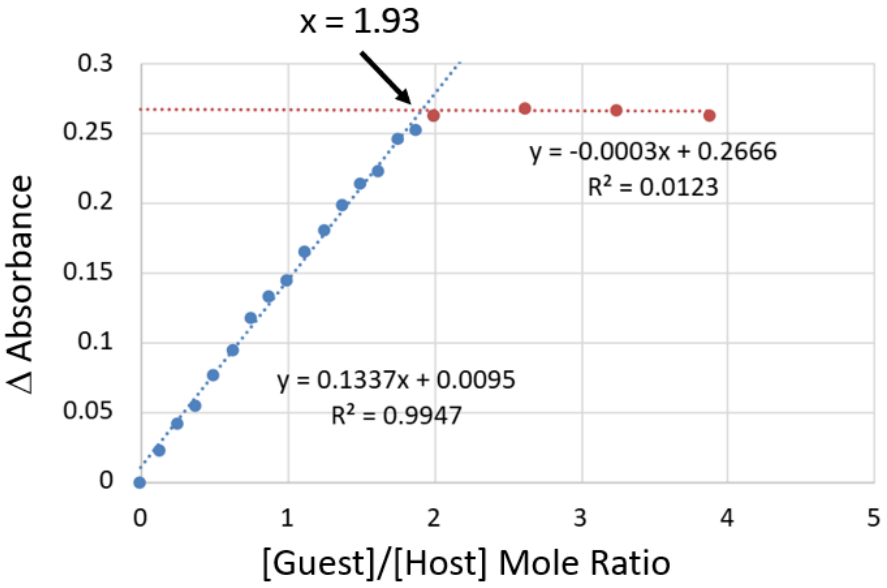

Fig. S35. Typical change in absorbance plotted against guest/host mole ratio for **1** binding to fluoride ion. The intercept at 1.93 suggests a 2:1 binding ratio. Analyses were carried out in triplicate for **1** binding with fluoride and *n*BuA providing a 90% CI range from 1.75 to 2.15 with an average of 1.93.

References

(1) SMART Version 5.630, SAINT+ Version 6.45. Bruker Analytical X-ray Systems, Inc., Madison, Wisconsin, USA, 2003.

(2) Sheldrick, G.M. *Acta Cryst*. **2008**, A64, 112-122.

(3) Kabalka, G. W.; Reddy, N. K.; Narayana, C., *Tetrahedron Lett.*, **1992**, *33*, 865-866.